

Coordinately regulated interbacterial antagonism defense pathways constitute a bacterial innate immune system

See-Yeon Ting¹, Kaitlyn D. LaCourse¹, Hannah E. Ledvina¹, Rutan Zhang², Matthew C. Radey¹,
Hemantha D. Kulasekara¹, Rahul Somavanshi¹, Savannah K. Bertolli¹, Larry A. Gallagher¹,
Jennifer Kim¹, Kelsi M. Penewit³, Stephen J. Salipante³, Libin Xu², S. Brook Peterson¹ and
Joseph D. Mougous^{1,4,5,*}

¹Department of Microbiology, University of Washington School of Medicine, Seattle, WA 98109, USA

²Department of Medicinal Chemistry, University of Washington School of Pharmacy, Seattle, WA 98195, USA

³Department of Laboratory Medicine and Pathology, University of Washington School of Medicine, Seattle, WA 98195

⁴Department of Biochemistry, University of Washington School of Medicine, Seattle, WA 98195, USA

⁵Howard Hughes Medical Institute, University of Washington, Seattle, WA 98195, USA

* To whom correspondence should be addressed: J.D.M.

Email – mougous@uw.edu

Telephone – (+1) 206-685-7742

1 **Abstract**

2 Bacterial survival is fraught with antagonism, including that deriving from viruses and
3 competing bacterial cells¹⁻³ ⁴. It is now appreciated that bacteria mount complex antiviral
4 responses; however, whether a coordinated defense against bacterial threats is undertaken is not
5 well understood. Previously we showed that *Pseudomonas aeruginosa* possess a danger sensing
6 pathway that is a critical fitness determinant during competition against other bacteria^{5,6}. Here,
7 we conducted genome-wide screens in *P. aeruginosa* that reveal three conserved and widespread
8 interbacterial antagonism resistance clusters (*arc1-3*). We find that although *arc1-3* are
9 coordinately activated by the Gac/Rsm danger sensing system, they function independently and
10 provide idiosyncratic defense capabilities, distinguishing them from general stress response
11 pathways. Our findings demonstrate that Arc3 family proteins provide specific protection against
12 phospholipase toxins by preventing the accumulation of lysophospholipids in a manner distinct
13 from previously characterized membrane repair systems. These findings liken the response of *P.*
14 *aeruginosa* to bacterial threats to that of eukaryotic innate immunity, wherein threat detection
15 leads to the activation of specialized defense systems.

16

17 Antagonism from other organisms is a threat faced nearly universally by bacteria living
18 in mixed populations, yet we are only beginning to understand the mechanisms employed in
19 defense against these assaults^{1,7,8}. One defense mechanism that is common in the gut microbiome
20 and potentially other habitats is the production of immunity proteins that grant protection against
21 specific toxins delivered by the type VI secretion system (T6SS)⁹. These “orphan” immunity
22 proteins share homology with and are likely evolved from cognate immunity proteins that protect
23 bacteria from undergoing self-intoxication, which is inherent to the indiscriminate nature of the
24 T6SS delivery mechanism. Core cellular structures have also been implicated in promoting
25 survival during interbacterial antagonism. Extracellular polysaccharide capsules protect *Vibrio*
26 *cholerae* and *E. coli* from T6SS-based attack of other species^{10,11}, and in *Acinetobacter*
27 *baumannii*, lysine modification at peptidoglycan crosslinks was suggested to render the cell wall
28 resistant to degradation by amidase toxins¹². Finally, characterized stress response pathways also
29 appear to contribute to antagonism defense. Indeed, it has been suggested that bacterial stress
30 responses evolved in part as a means of detecting and responding to antagonistic competitors
31 ^{13,14}. A candidate-based approach applied to *E. coli* and *P. aeruginosa* found that stress response
32 genes involved in envelope integrity and acid stress, among others can contribute to resistance
33 against a *V. cholerae* phospholipase toxin¹⁵. While the *P. aeruginosa* genes identified impacted
34 survival when the toxin was produced heterologously within the organism, they did not influence
35 the fitness of the bacterium during interbacterial competition with *V. cholerae*.

36 We previously discovered that *P. aeruginosa* mounts an effective, but largely undefined
37 defense upon exposure to an antagonistic competitor, which we named the *P. aeruginosa*
38 response to antagonism (PARA)⁵. The response is activated when a subpopulation of *P.*
39 *aeruginosa* cells are lysed, releasing intracellular contents that trigger the response in

40 neighboring survivors⁶. PARA is coordinated by the Gac/Rsm global regulatory pathway, which
41 posttranscriptionally controls the expression of nearly 400 genes^{16,17}. This regulon includes the
42 Hcp secretion island I-encoded type VI secretion system (H1-T6SS), the activity of which
43 enables *P. aeruginosa* to kill or disable competing bacteria through the delivery of a cocktail of
44 toxic effector proteins¹⁸. While an important component of PARA, data suggest that the H1-
45 T6SS is just one feature of the response; *P. aeruginosa* strains lacking functionality of the two-
46 component system required to initiate Gac/Rsm signaling are severely crippled in interbacterial
47 antagonism defense relative to those lacking only the H1-T6SS⁶. The majority the genes under
48 Gac/Rsm control encode proteins of unknown function and we hypothesized that these could
49 represent uncharacterized, novel mechanisms by which *P. aeruginosa* defends against
50 interbacterial antagonism.

51 Prior work by our laboratory has shown that *B. thailandensis* (*B. thai*) fiercely
52 antagonizes *P. aeruginosa* using its antibacterial T6SS⁵. Thus, to identify its interbacterial
53 defense factors, we subjected a transposon library of *P. aeruginosa* to antagonism by *B. thai* or a
54 derivative lacking antibacterial T6SS activity (Δ T6S) and used high-throughput sequencing to
55 measure gene-level fitness changes. Duplicate screening of this library revealed 34 genes critical
56 for the survival of *P. aeruginosa* specifically while undergoing antagonism by *B. thai* (Fig. 1A,
57 Supplemental Fig. 1A,B, Supplemental Table 1). Strikingly, 25 of these belong to the Gac/Rsm
58 regulon and three additional hits included genes directly involved in the Gac/Rsm signaling
59 system^{16,17}. Indeed, disruption of genes encoding GacS and GacA, the central sensor kinase and
60 response regulator required for activation of the pathway, respectively, elicited the strongest
61 interbacterial defense defect among all genes in the *P. aeruginosa* genome (Fig. 1A,B). On the

62 contrary, inactivating insertions in *retS*, encoding a hybrid sensor kinase that negatively regulates
63 GacS, increased interbacterial competitiveness.

64 Our screens identified previously uncharacterized genes belonging to three operons under
65 Gac/Rsm control¹⁶, several genes within two operons of the HSI-I-encoded T6SS (H1-T6SS)¹⁸,
66 and two genes within an operon not subject to Gac/Rsm regulation (Fig. 1C, Supplemental Fig.
67 1C, Supplemental Table 1). Given that false positives are less common among multiple gene hits
68 within an operon, we focused on these genes for subsequent validation in pairwise competition
69 assays. Strains bearing in-frame deletions of the genes most strongly hit in each operon showed
70 substantially reduced fitness in competition with *B. thai*, and in each instance this could be
71 partially restored by genetic complementation (Fig. 1D). Further consistent with our screening
72 results, the strains grew similarly to the wild-type in competition with *B. thai* ΔT6S (Fig. 1E).

73 The *P. aeruginosa* Gac/Rsm pathway has been implicated in a process we termed danger
74 sensing^{5,6}. We showed that the lysis of neighboring kin cells triggers the pathway, leading to
75 T6SS activation. However, the Gac/Rsm pathway posttranscriptionally activates hundreds of
76 genes whose function has largely remained cryptic (Fig. 1B). Bioinformatic analyses suggested
77 that each of the uncharacterized Gac/Rsm-regulated operons hit in our screen likely constitute a
78 discrete pathway. Five of the six genes within the PA2536-41 cluster are predicted to encode
79 proteins related to phospholipid biosynthesis or metabolism, including four genes encoding
80 products with significant homology to enzymes required for phosphatidylglycerol synthesis
81 (Supplemental Fig. 2A). Orthologs of core bacterial phospholipid biosynthetic machinery are
82 encoded elsewhere in the genome, indicating likely specialization of this putative pathway. The
83 PA4317-23 genes co-occur across many species within the Xanthomonadaceae and
84 Pseudomonadaceae (Supplemental Fig. 2B). While none of the proteins encoded by this gene

85 cluster have been characterized, they include a predicted MoxR-like AAA+-ATPase and a
86 protein with a Von Willebrand Factor (VWF) domain. Related protein pairs co-occur widely, and
87 are known to cooperate in a chaperone-like function that releases protein inhibition or stimulates
88 metal cofactor insertion^{19,20}. Finally, PA5113 and PA5114 also co-occur widely, and several
89 organisms encode single polypeptides that represent a fusion of the two proteins (Supplemental
90 Fig. 2C).

91 Next we sought to obtain experimental support for our hypothesis that the Gac/Rsm-
92 regulated operons hit in our screen constitute independent functional units. First, we compared
93 the fitness of our single deletion strains to those bearing in-frame deletions in the two genes most
94 strongly hit within each operon. In each operon, the second deletion did not impact
95 competitiveness with *B. thai*, indicative of an epistatic relationship (Supplemental Fig. 3A). On
96 the contrary, additive effects on interbacterial competitiveness were observed when genes from
97 each of the three operons were inactivated in a single strain. Indeed, the fitness deficiency of this
98 triple mutant strain approaches that of the $\Delta gacS$ strain, which lacks Gac/Rsm function entirely
99 (Supplemental Fig. 3B). Together, these data reveal that the Gac/Rsm pathway, and discrete
100 functional units under its control, are critical for *P. aeruginosa* survival when antagonized by the
101 T6SS of *B. thai*. Based on these data, we named the genes with the three Gac/Rsm-regulated
102 operons hit in our screen *arc1A-F* (antagonism resistance cluster 1, PA2536-41), *arc2A-G*
103 (PA4317-23) and *arc3A,B* (PA5113-14) (Fig. 1C).

104 As a first step toward understanding how Arc1-3 influence the competitiveness of *P.*
105 *aeruginosa*, we asked whether they serve defensive or offensive roles. In our initial screen, *B.*
106 *thai* dramatically outnumbered *P. aeruginosa* (~50:1); therefore, the diminished *P. aeruginosa*
107 viability observed under these conditions suggested each pathway can function defensively.

108 However, these conditions do not exclusively isolate the defensive contribution of the pathways.
109 For example, we observed that killing competitor cells via the H1-T6SS indirectly contributes to
110 *P. aeruginosa* viability under these conditions, likely by expanding the available growth niche.
111 To probe the capacity of Arc1-3 to antagonize *B. thai*, we initiated co-culture growth competition
112 assays with an excess of *P. aeruginosa*. Under these conditions, Arc2 and Arc3 had no impact on
113 *B. thai* survival, and Arc1 inactivation led to a modest reduction in *B. thai* survival relative to its
114 impact on *P. aeruginosa* defense (Fig. 2A). In contrast, the H1-T6SS reduced *B. thai* survival by
115 approximately four orders of magnitude, eclipsing its impact on *P. aeruginosa* defense by ~100-
116 fold. Together, these finding indicate that the contributions of Arc1-3 to *P. aeruginosa*
117 competitiveness during antagonism arise predominately from defensive mechanisms.

118 Our results suggested that the Gac/Rsm system functions analogously to innate immune
119 sensors of eukaryotic organisms, wherein danger sensing activates the expression of
120 independently functioning downstream effectors that defend the cell against specific threats²¹. By
121 extension, this response should be distinct from that provoked by general stressors. To test this,
122 we measured the contribution of Arc1-3 to *P. aeruginosa* survival in conditions known to induce
123 general stress response systems, including heat shock, exposure to H₂O₂, and propagation in high
124 salinity media or media containing detergent^{22,23}. Unlike previously established stress intolerant
125 control strains ($\Delta rpoS$ and $\Delta vacJ$), the survival of strains lacking Arc1-3 function was equivalent
126 to wild-type *P. aeruginosa* in these assays, suggesting that their function is distinct from those
127 involved in general stress resistance (Supplemental Fig. 4). This is also in-line with the
128 regulatory profile of Arc1-3; immunoblotting showed that basal expression each is exceedingly
129 low, yet highly inducible through stimulation of the antagonism responsive Gac/Rsm pathway
130 (Supplemental Fig. 5).

131 The specific involvement of Arc1-3 in defense against antagonism led us to hypothesize
132 that the pathways could grant protection against mechanistically distinct threats. Notably, *B. thai*
133 delivers a cocktail of toxins to target cells including two predicted phospholipases (Tle1 and
134 Tle3)²⁴, a peptidoglycan-degrading amidase (Tae2) and a colicin-like toxin predicted to form
135 inner membrane pores (ColA)^{25,26}. To determine the role of Arc1-3 in defense against insults
136 caused by toxins with biochemically diverse modes of action, we subjected strains with
137 individual Arc pathways inactivated to pairwise competition against *B. thai* strains lacking single
138 toxins in its arsenal. For Tle1 and Tle3, which are duplicated in the *B. thai* genome and required
139 for basal T6SS function, strains bearing mutated codons corresponding to predicted catalytic
140 residues of the proteins were utilized (Supplemental Fig. 6). Strikingly, we found that Tle3
141 inactivation abrogated the antagonism defense defect of *P. aeruginosa* lacking Arc3 function
142 (Fig. 2B), whereas its defense defect was maintained in competition experiments against other
143 toxin-inactivated strains of *B. thai*. In contrast, the survival of *P. aeruginosa* lacking Arc2
144 function was significantly restored by deletion of *colA* in *B. thai*, while none of the single
145 effector mutations within *B. thai* impacted the defense defect of *P. aeruginosa* lacking Arc1
146 function. These results support the hypothesis that Arc pathways can afford protection in a
147 manner specific to the damage arising from mechanistically distinct threats. *B. thai* delivers
148 toxins beyond those we inactivated in this study, therefore we cannot rule out that Arc1 – like
149 Arc2 and Arc3 – provides effector-specific defense.

150 We found that Arc2 and Arc3 are major defense factors against insults caused by ColA
151 and Tle3, respectively, suggesting that these toxins may damage cells by a mechanism not
152 efficiently countered by other cellular pathways. To evaluate the relative defensive contribution
153 of Arc2 and Arc3 genome-wide, we performed additional transposon-based screening in which a

154 mutant library of *P. aeruginosa* was grown in competition with *B. thai* strains lacking ColA or
155 Tle3 activity. Remarkably, this experiment defined *arc3B* as the gene most critical for *P.*
156 *aeruginosa* survival during intoxication by Tle3 (Fig. 2C, Supplemental Table 2). Insertions in
157 the second Arc3 gene, *arc3A*, also crippled *P. aeruginosa* defense against Tle3, though to a
158 lesser degree. Arc2 genes were dispensable for Tle3 defense, and only one gene within Arc1
159 contributed to Tle3 defense beyond the three-fold insertion frequency ratio cut-off we employed.
160 Inactivation of ColA had a relative minor impact on the fitness of most *P. aeruginosa* transposon
161 mutants (Figure 2D, Supplemental Table 3). However, four of the six Arc2 genes hit in our
162 initial screen provided defense against ColA that exceeded our three-fold cut-off. Additionally,
163 one Arc1 gene met these criteria, whereas Arc3 genes were wholly dispensable for defense
164 against ColA. These results support the model that Arc3 provides specific defense against Tle3,
165 Arc2 provides a degree of specific protection against ColA, and Arc1 serves a broader role in
166 antagonism defense. A comparison of the fitness contributions of each Arc pathway and the H1-
167 T6SS to *P. aeruginosa* undergoing intoxication by Tle3 or ColA highlights the degree of their
168 specificity (Fig. 2E).

169 The highly specific defense afforded by Arc3 against the predicted phospholipase Tle3
170 prompted us to further interrogate its function. Arc3B is a large protein containing 35 predicted
171 transmembrane domains and lacking residues strongly indicative of enzymatic activity (Fig. 3A).
172 With predicted outer-membrane anchored N-terminal lipidation and a C-terminal inner-
173 membrane transmembrane helix, Arc3A is expected to span the periplasm. Neither Arc3A nor
174 Arc3B share significant homology with characterized proteins; however, apparent orthologs of
175 each are encoded by neighboring open reading frames across an exceptionally wide distribution
176 of bacteria (Fig. 3B). Arc3B-related proteins are composed of domain of unknown function 2339

177 (DUF2339), possess large, yet varying numbers of transmembrane segments, and are found in
178 bacteria belonging to most Gram-negative and Gram-positive phyla. Consistent with the
179 predicted N-terminal localization of Arc3A to the outer-membrane, its related proteins are
180 restricted to Gram-negative phyla. Co-immunoprecipitation studies using epitope-tagged variants
181 of the Arc3A and Arc3B encoded at their native chromosomal loci provided evidence that the
182 two proteins stably associate (Supplemental Table 4). The *arc3A* and *arc3B* genes abut a third
183 gene encoded in the same orientation, *estA*, and there is evidence that transcripts containing all
184 three genes are generated by *P. aeruginosa*²⁷. Although *estA* encodes an esterase²⁸, which could
185 have relevance for phospholipase defense, *estA* was not detected in our co-immunoprecipitation
186 analyses, it did not exhibit differential insertion frequency in our screens, and in-frame deletion
187 of *estA* did not impact *P. aeruginosa* survival during intoxication by Tle3 (Supplemental Tables
188 1-3, Supplemental Fig. 7A).

189 The observation that Arc3B proteins are found in bacteria lacking an Arc3A homolog,
190 combined with our finding that Arc3A contributes relatively little to Tle3 defense, led us to
191 speculate that Arc3B plays an intrinsic role in defense, independent of its interaction Arc3A. We
192 tested this by examining the ability of Arc3B-related proteins to complement the defense defect
193 of *P. aeruginosa* Δ *arc3B*. Despite high sequence divergence that would likely preclude specific
194 interactions with Arc3A or other *P. aeruginosa* factors, four of these proteins restored Tle3
195 defense to a statistically significant degree and two provided protection equivalent to that of *P.*
196 *aeruginosa arc3B* expressed in the same manner (Fig. 3C). We also examined one of these
197 proteins in its native context. Inactivation of *arc3B* in *P. protegens* conferred a strong
198 interbacterial antagonism defense defect specific to *B. thai* Tle3 (Fig. 3D). In total, these data
199 strongly suggest that proteins in the Arc3B family possess the intrinsic capacity to protect

200 bacteria against interbacterial phospholipase toxins. While we find that Arc3A also participates
201 in defense (Figs. 1A, 2C, Supplemental Table 1,2), these data suggest that its role is auxiliary.

202 Enzymes with PLA activity cleave glycerophospholipids at the *sn1* or *sn2* position,
203 generating fatty acid and detergent-like lysophospholipid products²⁹. For toxins like Tle3, which
204 are delivered to target cells in exceedingly low quantities^{30,31}, it is likely toxic products, rather
205 than phospholipid depletion *per se*, that most immediately contribute to cell death. Based on the
206 intrinsic capacity of Arc3B to grant protection against Tle3, a predicted PLA, we hypothesized
207 that it directly mitigates damage caused by the toxic products of Tle3. To test this, we measured
208 phospholipid content within extracts derived from competing *P. aeruginosa* and *B. thai* strains at
209 a time point immediately prior to detectable changes in *P. aeruginosa* viability. Strikingly,
210 relative to mixtures containing the wild-type organisms, those containing *P. aeruginosa* Δ arc3B
211 possessed highly elevated levels of lysophosphatidylethanolamine (LPE) and
212 monolysocardiolipin (MLCL) in a manner dependent on the activity of Tle3 in *B. thai* (Fig. 4A).
213 Lysophosphatidylglycerol, free fatty acid, and corresponding parent phospholipid levels were not
214 measurably altered by Tle3 (Supplemental Fig. 8A,B).

215 The accumulated lysophospholipids we observed could derive from *P. aeruginosa* or they
216 could result from retaliatory activity against *B. thai*. To distinguish these possibilities, we
217 subjected *P. aeruginosa* strains with radiolabeled phospholipids to Tle3 intoxication by
218 unlabeled *B. thai* strains. Radiographic TLC analysis of the phospholipids generated in these
219 strain competition mixtures confirmed that *P. aeruginosa* lacking Arc3B accumulates LPE and
220 MLCL during Tle3 intoxication (Fig. 4B-D). Tle3 belongs to a family of effectors for which
221 there remains no definitively characterized member. We were unable to measure the activity of
222 the enzyme in vitro; thus, to determine whether the accumulation of LPE and MLCL were a

223 direct result of Tle3 activity, we quantified phospholipids in extracts derived from *B. thai* strains
224 undergoing Tle3-based self-intoxication (Supplemental Fig. 7B). Samples derived from mixtures
225 composed of a strain with Tle3 and a strain sensitized to Tle3 intoxication through cognate
226 immunity gene inactivation accumulated LPE and MLCL, mirroring our interspecies competition
227 findings (Fig. 4E).

228 In *E. coli*, lysophospholipids are transported across the inner membrane by the dedicated
229 transporter LpIT, after which they are reacylated by Aas³². Both LpIT and Aas have been shown
230 to play a critical role in defending *E. coli* cells from phospholipase attack³³. In *P. aeruginosa*,
231 LpIT and the acylation domain of Aas are found in a single predicted polypeptide, encoded by
232 PA3267 (*aas*). Interestingly, the *aas* gene was illuminated as a potential *P. aeruginosa*
233 antagonism defense factor in two of the transposon mutant screens we performed and *aas* genes
234 neighbor *arc3* genes in many bacteria (Fig. 2C, Supplemental Fig. 1B, Supplemental Fig. 9,
235 Supplemental Tables 1,2). In pairwise interbacterial competition assays we were unable to detect
236 the impact of *aas* inactivation on *P. aeruginosa* fitness; however, we found that *P. aeruginosa*
237 strains lacking both *aas* and *arc3B* exhibited a Tle3 defense defect substantially greater than that
238 associated with Arc3B inactivation alone (Fig. 4F). Additionally, we found that Aas is required
239 for PE regeneration from LPE, whereas Arc3B did not contribute to this process (Fig. 4G). These
240 findings indicate that *arc3* encodes a previously undescribed, widespread and independent
241 pathway that prohibits lysophospholipid accumulation by an interbacterial phospholipase toxin.

242 Evidence suggests that the existence of bacteria is characterized by an onslaught of
243 challenges to their integrity^{1,2}. This is borne out in-part by recent work in the phage arena, which
244 has highlighted a vast number of dedicated bacterial defense systems against these parasites^{3,4}. It
245 is now appreciated that the amalgam of these systems constitutes a bacterial immune system,

246 with both innate and adaptive arms that are functionally analogous, and even evolutionarily
247 related to those of eukaryotic organisms³⁴. Our work shows that bacteria also possess a multitude
248 of coordinately regulated pathways dedicated to defense against the threats posed by other
249 bacteria. This further cements the analogy between the immune systems of bacterial and
250 eukaryotic cells, the latter of which also rely on the coordinated production of factors specialized
251 for countering threats of viral or bacterial origin.

252 We found that Arc3B is the single cellular factor of *P. aeruginosa* most critical for
253 defense against a PLA toxin. Whether Arc3B, perhaps in concert with Arc3A, offer a wider
254 breadth of defensive activity is not known. However, it is notable that phospholipase toxins are
255 ancient and among the most prevalent bacterial toxins known. Even in the absence of direct
256 antagonism by a PLA toxin, environmental lysophospholipids and those generated during normal
257 cellular processes may represent ongoing threats to bacterial viability³⁵. We observed low
258 Arc3B expression in the absence of Gac/Rsm activation, arguing that its role in PARA serves an
259 adaptive purpose.

260 The precise mechanism by which Arc3 proteins defend against intoxication by
261 phospholipase toxins remains unknown. Although we found that Arc3 grants specific protection
262 against Tle3, the relatively low levels of *P. aeruginosa* intoxication achieved by Tle1 does not
263 permit us to rule out that it might also provide broader phospholipase defense. The number and
264 density of transmembrane helices in Arc3B family proteins is unusual and we postulate that these
265 anomalous features of the protein are intimately connected to its mechanism of action. These
266 segments may sequester lysophospholipids and facilitate their turnover or it is conceivable that
267 they directly recruit and interfere with phospholipase enzymes.

268 We have found that several previously uncharacterized gene clusters under Gac/Rsm
269 control contribute critically to PARA. Our bioinformatic analyses show that the *arc* clusters are
270 widely conserved among Bacteria, yet the Gac/Rsm pathway is restricted to γ -Proteobacteria. If
271 *arc* genes play similar roles in these diverse bacteria, which our data suggest, their expression is
272 also likely subject to induction by antagonism. It will be of interest in future studies to probe the
273 generality of coordinated interbacterial defenses by identifying additional signaling systems
274 responsive to antagonism. Collectively, our findings provide new insight into the diversity of
275 mechanisms bacteria have evolved to defend against interbacterial attack and suggest that many
276 more cryptic specialized defense pathways await discovery.

277 **Methods**

278 **Bacterial strains and culture conditions**

279 A detailed list of all strains and plasmids used in this study can be found in Supplemental
280 Table 5. Bacterial strains under investigation in this study were derived from *Pseudomonas*
281 *aeruginosa* PAO1, *Burkholderia thailandensis* E264, and *Pseudomonas protegens* pf-5³⁶⁻³⁸. All
282 strains were grown in Luria-Bertani (LB) broth and incubated either at 37°C (*P. aeruginosa* and
283 *B. thai*) or 30°C (*P. protegens*). For *Pseudomonas* strains the media was supplemented with 25
284 µg ml⁻¹ irlgasan, 15 µg ml⁻¹ gentamicin, 5% (w/v) sucrose, and 0.2% (w/v) arabinose as needed.
285 *B. thai* was cultured with 15 µg ml⁻¹ gentamicin and 200 µg ml⁻¹ trimethoprim as necessary, and
286 counter-selection for allelic exchange was performed on M9 minimal medium agar plate
287 containing 0.4% (w/v) glucose and 0.2% (w/v) *p*-chlorophenylalanine. *Escherichia coli*
288 strains used in this study included DH5α for plasmid maintenance, SM10 for conjugal transfer of
289 plasmids into *P. aeruginosa*, *P. protegens*, and *B. thai*, and UE54 for radiolabeled
290 phosphatidylethanolamine (PE) synthesis. *E. coli* strains were grown in LB supplemented with
291 15 µg ml⁻¹ gentamicin, 150 µg ml⁻¹ carbenicillin, and 200 µg ml⁻¹ trimethoprim as needed.

292

293 **Plasmid construction**

294 All primers used in plasmid construction and generation of mutant strains are listed in
295 Supplemental Table 5. In-frame chromosomal deletions and point mutations were created using
296 the suicide vector pEXG2 for *P. aeruginosa* and *P. protegens*, and pJRC115 for *B. thai*^{39,40}. For
297 the generation of chromosomal mutation constructs, 750 bp regions flanking the mutation site
298 were PCR amplified and inserted stitched together into the appropriate vector via Gibson
299 assembly⁴¹. Site-specific chromosomal insertions in *P. aeruginosa* were generated using pUC18-

300 Tn7t-pBAD-araE as previously described⁴². Our trimethoprim-resistant *B. thai* strain was
301 generated using pUC18T-mini-Tn7-Tp-PS12-mCherry via the mini-Tn7 system⁴³.

302

303 **Generation of mutant strains**

304 For *P. aeruginosa* and *P. protegens* strain generation: pEXG2 mutation constructs were
305 transformed into *E. coli* SM10, and SM10 donors were subsequently mixed and incubated
306 together with *Pseudomonas* recipients on a nitrocellulose membrane on top of an LB agar plate
307 at a ratio of 10:1 donor–recipient. The cell mixtures were incubated for 6 hours at 37°C to allow
308 for conjugation. These cell mixtures were then scraped up, resuspended into 200 µl LB, and
309 plated on LB agar plates containing irgasan and gentamicin to select for cells containing the
310 mutant construct inserted into the chromosome. *Pseudomonas* merodiploid strains were then
311 grown overnight in non-selective LB media, followed by counter selection on LB no salt agar
312 plates supplemented with sucrose. Gentamicin sensitive, sucrose resistant colonies were screened
313 for allelic replacement by colony PCR and mutations were confirmed via Sanger sequencing of
314 PCR products.

315 For *B. thai* strain generation, pJRC115 mutation constructs were transformed into *E. coli*
316 SM10. Conjugation to enable plasmid transfer was performed as described above and plated on
317 LB agar containing gentamicin and trimethoprim to select for *B. thai* with the chromosomally
318 integrated plasmid. Merodiploids were grown overnight in LB media at 37°C, then plated on M9
319 minimal medium containing *p*-chlorophenylalanine for counter selection. Trimethoprim
320 sensitive, *p*-chlorophenylalanine resistant colonies were screened for allelic replacement by
321 colony PCR and mutations were confirmed via Sanger sequencing of PCR products.

322 For expression of Arc1F, Arc2G, Arc3B, and Arc3B-homologs in *P. aeruginosa*, pUC18-
323 Tn7t-pBAD-araE containing the gene of interest and the helper plasmid pTNS3 were co-
324 transformed into *P. aeruginosa* strains by electroporation⁴⁴. After 6 hours of outgrowth in LB at
325 37°C, transformants were plated on a LB agar plate with gentamycin to select for cells with
326 mini-Tn7 integration.

327

328 ***Bacterial competition assay***

329 For each co-culture competition experiment, donor and recipient strains were first grown
330 for 20 hours in LB medium. Cultures were spun for 1 min at 20,000 g to pellet cells, the
331 supernatant removed, and cells were washed once with fresh LB medium. Cell pellets were
332 resuspended in LB and normalized to OD₆₀₀ = 20. Mixtures of donor and recipient strains were
333 then established at 20:1 (*B. thai* vs. *P. aeruginosa*, *P. protegens*, or *B. thai*) or 10:1 (*P.*
334 *aeruginosa* vs. *B. thai*) v/v ratios. The initial ratios of donor and recipient strains in these
335 mixtures were measured by performing 10-fold serial dilutions and plating on appropriate
336 selective media to evaluate by colony forming unit (CFU) analysis. The co-culture competitions
337 were initiated by spotting 5 ul of each mixture onto nitrocellulose filters placed on 3% (w/v) agar
338 LB no salt plates supplemented with L-arabinose for induction of gene-expression as necessary.
339 Competitions were incubated for 6 hours at 37°C between *B. thai* and *P. aeruginosa*, or 6 hours
340 at 30°C for competition between *B. thai* and *P. protegens*. For *B. thai* self-intoxication,
341 competitions were incubated at 37°C for 3 hours. Cells were harvested by scraping individual
342 spots from excised sections of the nitrocellulose filter into LB medium. Suspensions were
343 serially diluted and plated on selective media for CFU quantification.

344

345 **Immunoblotting analysis**

346 To analyze the expression of Arc1F-VSV-G, Arc2G-VSV-G, and Arc3B-VSV-G, *P.*
347 *aeruginosa* strains were grown in LB broth at 37°C to log phase. Cells were pelleted and
348 resuspended in lysis buffer (20 mM Tris-HCl, pH 7.5, 300 mM NaCl, 10% (v/v) glycerol) and
349 then mixed 1:1 with 2X SDS-PAGE sample loading buffer. Samples were then boiled at 100°C
350 for 10 minutes and loaded at equal volumes to resolve using SDS-PAGE, then transferred to
351 nitrocellulose membranes. Membranes were blocked in TBST (10 mM Tris-HCl pH 7.5, 150
352 mM NaCl, and 0.1% (w/v) Tween-20) with 5% (w/v) non-fat milk for 30 minutes at room
353 temperature, followed by incubation with anti-VSV-G or with anti-ribosome polymerase β
354 subunit primary antibodies diluted in TBST for 1 hour at room temperature on an orbital shaker.
355 Blots were then washed with TBST, followed by incubation with secondary antibody (Goat anti-
356 Rabbit or anti-Mouse HRP conjugated) diluted in TBST for 30 minutes at room temperature.
357 Finally, blots were washed with TBST again and developed using Radiance HRP substrate and
358 visualized using iBright imager.

359

360 **Lipidomic analysis**

361 To analyze lipid content after intra- and inter-species intoxication, overnight cultures of
362 donor and recipient cells were harvested and mixed at 1 : 1 (v/v) ratio in LB medium. These
363 mixtures were spotted onto a 3% (w/v) agar LB no salt plate, and incubated for 1 hour at 37°C to
364 allow for intoxication. Cells were then collected, and the lipids were extracted using the Bligh-
365 Dyer method⁴⁵. Briefly, bacterial pellets were resuspended in 0.5 mL of solution containing 0.5
366 M NaCl in 0.5 N HCl, followed by adding 1.5 mL of chloroform/methanol mixture (1:2, v/v).
367 Suspensions were vortexed at room temperature for 15 minutes, 1.5 mL of 0.5 M NaCl in 0.5 N

368 HCl solution was added to each sample, and vortexed for an additional 5 minutes. Lipid and
369 aqueous layers were separated by centrifugation at 2,000 g for 5 minutes. The lower lipid phase
370 was collected, and these dried lipid samples were analyzed for PE, PG, CL, LPE, LPG, and
371 MLCL content by the Kansas State Lipidomics Research Center.

372 Lipid samples were analyzed by electrospray ionization triple quadrupole mass
373 spectrometry in direct infusion mode, and data were processed as described by with slight
374 modifications⁴⁶, which include use of a Waters Xevo TQS mass spectrometer (Milford, MA).
375 Internal standards used to normalize data are shown in Supplemental Table 6. For PE and LPE,
376 SPLASH standards were used for normalization (Avanti Polar Lipids, Alabaster, AL). Mass
377 spectrometry global parameters, scan modes, and data processing parameters are shown in
378 Supplemental Table 6.

379

380 **Proteomic analysis**

381 *P. aeruginosa* strains containing VSV-G-tagged proteins were grown in 50 mL to mid-log
382 phase, centrifuged at 2,500 g for 15 minutes, and the pellets harvested by resuspension in lysis
383 buffer (20 mM Tris-HCl pH 7.5, 300 mM NaCl, 5% (w/v) glycerol, 0.5% (v/v) Triton X-100).
384 Cell lysates were prepared by sonication, and tagged proteins were enriched by incubating cell
385 lysates with 30 µl of anti-VSV-G agarose beads at 4°C for 4 hours with constant rotation.
386 Agarose beads were then pelleted by centrifugation at 100 g for 2 minutes, and washed 3 times
387 with 20 mM ammonium bicarbonate. VSV-G agarose beads and bound proteins were then
388 treated with 10 µl of 10 ng/µl (100 ng total per sample) sequencing grade trypsin for 16 hours at
389 37°C. After digestion, 40 µl of 20 mM ammonium bicarbonate was added to the agarose beads
390 and peptide mixture and lightly mixed. Beads were centrifuged at 300 g for 3 minutes, and the

391 supernatant collected as the peptide fraction. This peptide mixture was reduced with 5 mM
392 Tris(2-carboxyethyl) phosphine hydrochloride for 1 hour, followed by alkylation using 14 mM
393 iodoacetamide for 30 minutes in the dark at room temperature. Alkylation reactions were
394 quenched using 5 mM 1,4-Dithiothreitol. Samples were then diluted with 100% acetonitrile
395 (ACN) and 10% (w/v) trifluoroacetic acid (TFA) to a final concentration of 5% ACN (v/v) and
396 0.5% TFA (w/v) and applied to MacroSpin C18 columns (30 μ g capacity) that had been charged
397 with 100% acetonitrile and ddH₂O. Bound peptides were then washed twice in 5% (v/v) ACN
398 and 0.5% (w/v) TFA, before elution with 70% (v/v) ACN and 0.1% (v/v) formic acid (FA).

399 Peptides were analyzed by LC-MS/MS using a Dionex UltiMate 3000 Rapid Separation
400 nanoLC and a Q ExactiveTM HF Hybrid Quadrupole-OrbitrapTM Mass Spectrometer (Thermo
401 Fisher Scientific Inc, San Jose, CA). Approximately 1 μ g of peptide samples was loaded onto the
402 trap column, which was 150 μ m \times 3 cm in-house packed with 3 μ m C18 beads. The analytical
403 column was a 75 μ m \times 10.5 cm PicoChip column packed with 3 μ m C18 beads (New Objective,
404 Inc. Woburn, MA). The flow rate was kept at 300 nL/minute. Solvent A was 0.1% FA in water
405 and Solvent B was 0.1% FA in ACN. The peptide was separated on a 120-minute analytical
406 gradient from 5% ACN/0.1% FA to 40% ACN/0.1% FA. The mass spectrometer was operated in
407 data-dependent mode. The source voltage was 2.10 kV and the capillary temperature was 320
408 degrees C. MS 1 scans were acquired from 300–2000 m/z at 60,000 resolving power and
409 automatic gain control (AGC) set to 3×10^6 . The top 15 most abundant precursor ions in each MS
410 1 scan were selected for fragmentation. Precursors were selected with an isolation width of 2 Da
411 and fragmented by Higher-energy collisional dissociation (HCD) at 30% normalized collision
412 energy in the HCD cell. Previously selected ions were dynamically excluded from re-selection
413 for 20 seconds. The MS 2 AGC was set to 1×10^5 .

414 Proteins were identified from the tandem mass spectra extracted by Xcalibur version 4.0.
415 MS/MS spectra were searched against the Uniprot *P. aeruginosa* PAO1 strain database using
416 Mascot search engine (Matrix Science, London, UK; version 2.5.1). The MS 1 precursor mass
417 tolerance was set to 10 ppm and the MS 2 tolerance was set to 0.05 Da. A 1% false discovery
418 rate cutoff was applied at the peptide level. Only proteins with a minimum of two unique
419 peptides above the cutoff were considered for further study. The search result was visualized by
420 Scaffold (version 4.8.3. Proteome Software, INC., Portland, OR).

421

422 **Transposon mutant library construction**

423 A *P. aeruginosa* PAO1 transposon mutant library of ~80,000 unique *Himar1* insertions
424 was prepared using established protocols⁴⁷. Briefly, *P. aeruginosa* were mutagenized by delivery
425 of the transposon- and transposase-bearing suicide vector pBT20 from *E. coli* SM10 λpir⁴⁸.
426 Insertion mutants were selected on LB agar containing irgasan and gentamycin and pooled. The
427 library was harvested and transposon insertion sites of the complete pool were defined by
428 transposon insertion sequencing as described below.

429

430 **Transposon mutant library screen in bacterial competition**

431 The *P. aeruginosa* transposon mutant library was grown at 37°C to mid-log phase. Cell
432 suspensions were then normalized to OD₆₀₀ = 1 and incubated with 100 OD₆₀₀ of *B. thai* donor
433 strains (wild type, $\Delta icmF$, $tle3^{S264A}$, or $\Delta colA$). Competitions were performed on 3% (w/v) agar
434 LB no salt plates at 37°C for 7 hours. Cells were washed once with PBS, diluted, and plated on
435 LB agar plates supplemented with irgsan to select for viable *P. aeruginosa* cells. After overnight

436 incubation, cells were harvested, and genomic DNA was directly extracted from pellets using
437 Qiagen Blood and Tissue Midi gDNA prep kit. Transposon insertion sequencing libraries were
438 generated from 3 µg gDNA per sample using the C-tailing method as described⁴⁹ with the
439 transposon-specific primers listed in Supplemental Table 5. For PCR round 1, PCR_1A and
440 PCR_1B were used. For PCR round 2, PCR_2A, PCR_2B, and PCR_2C were used. For
441 sequencing, Seq_primer was used. Libraries were pooled and sequenced in multiplex using an
442 Illumina MiSeq with a 5% PhiX spike-in.

443

444 **Tn-Seq data analysis**

445 Seqmagick was used to trim the first six bases from each read
446 (<https://github.com/fhcrc/seqmagick>). Reads were then aligned, and counts were enumerated
447 using TRANSIT TPP (<https://transit.readthedocs.io/en/latest/tpp.html>). An annotation GFF was
448 created from the original *P. aeruginosa* PAO1 GFF file (GCF_000006765.1) and was translated
449 to TRANSIT portable format using the TRANSIT 'convert gff_to_prot_table' command
450 (https://transit.readthedocs.io/en/latest/transit_running.html#prot-tables-annotations). Finally, the
451 TRANSIT 'export combined_wig' command was used to combine and annotate the counts.
452 Supplementary Table S7 provides summary data of the sequencing runs and their processing by
453 TRANSIT.

454

455 **Bioinformatic analysis of Arc3 genes distribution**

456 The phylogenetic profiler tool in IMG⁵⁰ was used to determine the distribution of Arc3B
457 homologs (identified as proteins classified under the Pfam 10101) across bacterial phyla. The
458 number and location of predicted transmembrane domains present in representative Arc3B

459 homologs from each phylum was calculated using CCTOP and TMpred (, https://embnet.vital-it.ch/software/TMPRED_form.html)⁵¹. Homologs of Arc3A encoded adjacent to Arc3B-like
460 genes were identified on the basis of their classification in the Pfam 13163.
461
462

463 **Stress resistance assay**

464 *P. aeruginosa* cultures were assayed for the ability to survive oxidative stress (50 mM
465 H₂O₂), heat stress (55°C), osmotic stress (3 M NaCl), and detergent stress (0.5% (w/v) SDS and
466 0.25 mM EDTA) in LB media as previously described with modifications²². After incubation
467 with the oxidative, heat and osmotic stress conditions, cultures were serially diluted 10-fold in
468 LB medium and plated on LB agar for subsequent analysis of remaining viable cells by CFU
469 determination. For oxidative stress, stationary-phase cultures were diluted to OD₆₀₀ = 0.1 and
470 incubated in LB media containing 50 mM H₂O₂ for 30 minutes at 37°C with continuous shaking.
471 For heat stress, stationary-phase cultures were diluted in pre-warmed LB media to OD₆₀₀ = 0.1
472 and incubated at 55°C for 30 minutes with continuous shaking. For osmotic stress, overnight
473 cultures were diluted in LB media containing 3 M NaCl to OD₆₀₀ = 0.1. Cultures were incubated
474 at 37°C for 20 hours with shaking. For detergent stress, cultures were serially diluted in LB
475 media and directly plated on LB agar plates containing 0.5% (w/v) SDS and 0.25 mM EDTA for
476 CFU quantification.

477

478 **Thin Layer Chromatography - Phospholipid analysis**

479 To prepare [³²P]-labeled bacteria, *P. aeruginosa* strains were grown in LB media
480 supplemented with 5 µCi/ml [³²P]-orthophosphoric acid. Tle3 intoxication was performed by
481 mixing 200 OD₆₀₀ of *B. thai* and [³²P]-*P. aeruginosa* at a 10 : 1 ratio (v/v) and incubating this

482 mixture at 37°C for 1 hour on 3% (w/v) agar LB no salt plates containing L-arabinose as
483 necessary. After 1 hour of intoxication, cells were collected, and the lipids were extracted using
484 the Bligh-Dyer method as described above. Purified lipid samples were loaded onto a silica gel
485 thin-layer plate and developed with chloroform/methanol/acetic acid/ddH₂O (85:15:10:3.5,
486 v/v/v/v) solvent system⁵². The air-dried plate was exposed to a storage phosphor screen.
487 Individual phospholipid was visualized and quantified using phosphorimaging to calculate
488 phospholipid content expressed as mol % of the total phospholipid pool.

489

490 **PE regeneration assay**

491 To generate [³²P]-labeled PE, *E. coli* UE54 strain was grown in LB media supplemented
492 with 5 µCi/ml [³²P]-orthophosphate overnight at 37°C⁵³. Cells were collected and the lipids were
493 extracted using the Bligh-Dyer method as described above. The extracted lipids were dried and
494 resuspended in buffer containing 100 mM HEPES-NaOH, pH=7.5, 100 mM KCl, 10 mM CaCl₂,
495 and 1% (w/v) n-Dodecyl-β-D-Maltoside. 10 units of pancreas Phospholipase A₂ were added to
496 digest PE to LPE at 37°C overnight with shaking. After incubation, lipids were extracted and
497 loaded onto a silica gel thin-layer plate and developed with chloroform/methanol/acetic
498 acid/ddH₂O (85:15:10:3.5, v/v/v/v) solvent system. The dried plate was exposed to an x-ray film
499 for 2 hours. The phospholipid bands were visualized by developing the film, and bands
500 corresponding [³²P]-LPE on the TLC plate were scraped, extracted, and resuspended in 100%
501 ethanol.

502 *P. aeruginosa* spheroplasts were generated by resuspending log-phase culture in 25 mM
503 Tris-HCl, pH 8, 450 mM sucrose, and 1.4 mM EDTA. After addition of 20 µg ml⁻¹ lysozyme,
504 cells were incubated on ice for 30 minutes. Intact spheroplasts were collected by centrifugation

505 (3,000 g for 5 minutes) at 4°C and gently resuspended in 25 mM Tris-HCl, pH 8, and 450 mM
506 sucrose. To examine PE regeneration, [³²P]-LPE was added into spheroplast solutions and
507 incubated at 37°C. The reactions were terminated at the indicated time by adding chloroform-
508 methanol mixture (1:2, v/v). The lipids were extracted, separated by TLC, and analyzed using
509 phosphorimaging as described above⁵⁴.

510

511 **Data availability**

512 Sequence data associated with this study is available from the Sequence Read Archive at
513 BioProject PRJNA754428 (<http://www.ncbi.nlm.nih.gov/bioproject/754428>).

514 **Acknowledgements**

515 We thank Simon Dove, Josh Woodward, Lei Zheng and Mougous laboratory members
516 for helpful discussions, Mikhail Bogdanov and Lei Zheng for sharing reagents, and Colin Manoil
517 and Jason Smith for sharing equipment. This work was supported by the grants from NIH
518 (AI080609 to J.D.M., DK089507 to S.J.S., and R01AI136979 to L.X.) and the Cystic Fibrosis
519 Foundation (SINGH19R0). Equipment utilized was supported by the Office of the Director,
520 National Institutes of Health under award number S10OD026741. JDM is an HHMI Investigator.

521

522 **Competing interests**

523 The authors declare no competing interests.

524

525 **Author contributions**

526 S.-Y.T., K.D.L., H.E.L., S.B.P. and J.D.M. designed the study, S.-Y.T., K.D.L., H.E.L.,
527 R.Z., H.D.K., R.S., S.K.B., L.A.G., J.K., K.M.P., and S.J.S. performed experiments, S.-Y.T.,
528 K.D.L., H.E.L., M.C.R., L.X., S.B.P., and J.D.M. analyzed data, and S.-Y.T., S.B.P., and J.D.M.
529 wrote the manuscript with input from the other authors.

530

531 **Author Information**

532 Correspondence and requests for materials should be addressed to J.D.M.
533 (mougous@u.washington.edu).

References

- 1 Peterson, S. B., Bertolli, S. K. & Mougous, J. D. The Central Role of Interbacterial Antagonism in Bacterial Life. *Curr Biol* **30**, R1203-R1214, doi:10.1016/j.cub.2020.06.103 (2020).
- 2 Granato, E. T., Meiller-Legrand, T. A. & Foster, K. R. The Evolution and Ecology of Bacterial Warfare. *Curr Biol* **29**, R521–R537, doi:10.1016/j.cub.2019.04.024 (2019).
- 3 Hampton, H. G., Watson, B. N. J. & Fineran, P. C. The arms race between bacteria and their phage foes. *Nature* **577**, 327–336, doi:10.1038/s41586-019-1894-8 (2020).
- 4 Bernheim, A. & Sorek, R. The pan-immune system of bacteria: antiviral defence as a community resource. *Nat Rev Microbiol* **18**, 113-119, doi:10.1038/s41579-019-0278-2 (2020).
- 5 LeRoux, M. *et al.* Kin cell lysis is a danger signal that activates antibacterial pathways of *Pseudomonas aeruginosa*. *Elife* **4**, doi:10.7554/elife.05701 (2015).
- 6 LeRoux, M., Peterson, S. B. & Mougous, J. D. Bacterial danger sensing. *J Mol Biol* **427**, 3744–3753, doi:10.1016/j.jmb.2015.09.018 (2015).
- 7 Robitaille, S., Trus, E. & Ross, B. D. Bacterial Defense against the Type VI Secretion System. *Trends Microbiol* **29**, 187-190, doi:10.1016/j.tim.2020.09.001 (2021).
- 8 Hersch, S. J., Manera, K. & Dong, T. G. Defending against the Type Six Secretion System: beyond Immunity Genes. *Cell Rep* **33**, 108259, doi:10.1016/j.celrep.2020.108259 (2020).
- 9 Ross, B. D. *et al.* Human gut bacteria contain acquired interbacterial defence systems. *Nature* **575**, 224–228, doi:10.1038/s41586-019-1708-z (2019).
- 10 Hersch, S. J. *et al.* Envelope stress responses defend against type six secretion system attacks independently of immunity proteins. *Nat Microbiol* **5**, 706–714, doi:10.1038/s41564-020-0672-6 (2020).
- 11 Toska, J., Ho, B. T. & Mekalanos, J. J. Exopolysaccharide protects *Vibrio cholerae* from exogenous attacks by the type 6 secretion system. *Proc Natl Acad Sci U S A* **115**, 7997–8002, doi:10.1073/pnas.1808469115 (2018).
- 12 Le, N. H. *et al.* Peptidoglycan editing provides immunity to *Acinetobacter baumannii* during bacterial warfare. *Sci Adv* **6**, eabb5614, doi:10.1126/sciadv.abb5614 (2020).
- 13 Lories, B. *et al.* Biofilm Bacteria Use Stress Responses to Detect and Respond to Competitors. *Curr Biol* **30**, 1231-1244 e1234, doi:10.1016/j.cub.2020.01.065 (2020).
- 14 Cornforth, D. M. & Foster, K. R. Competition sensing: the social side of bacterial stress responses. *Nat Rev Microbiol* **11**, 285–293, doi:10.1038/nrmicro2977 (2013).

15 Kamal, F. *et al.* Differential Cellular Response to Translocated Toxic Effectors and Physical Penetration by the Type VI Secretion System. *Cell Rep* **31**, 107766, doi:10.1016/j.celrep.2020.107766 (2020).

16 Goodman, A. L. *et al.* A signaling network reciprocally regulates genes associated with acute infection and chronic persistence in *Pseudomonas aeruginosa*. *Dev Cell* **7**, 745–754 (2004).

17 Lapouge, K., Schubert, M., Allain, F. H. & Haas, D. Gac/Rsm signal transduction pathway of gamma-proteobacteria: from RNA recognition to regulation of social behaviour. *Molecular microbiology* **67**, 241–253 (2008).

18 Hood, R. D. *et al.* A type VI secretion system of *Pseudomonas aeruginosa* targets a toxin to bacteria. *Cell Host Microbe* **7**, 25–37 (2010).

19 Snider, J. & Houry, W. A. MoxR AAA+ ATPases: a novel family of molecular chaperones? *J Struct Biol* **156**, 200–209, doi:10.1016/j.jsb.2006.02.009 (2006).

20 Tsai, Y. C. *et al.* Insights into the mechanism and regulation of the CbbQO-type Rubisco activase, a MoxR AAA+ ATPase. *Proc Natl Acad Sci U S A* **117**, 381–387, doi:10.1073/pnas.1911123117 (2020).

21 Paludan, S. R., Pradeu, T., Masters, S. L. & Mogensen, T. H. Constitutive immune mechanisms: mediators of host defence and immune regulation. *Nature reviews. Immunology* **21**, 137–150, doi:10.1038/s41577-020-0391-5 (2021).

22 Jorgensen, F. *et al.* RpoS-dependent stress tolerance in *Pseudomonas aeruginosa*. *Microbiology (Reading)* **145** (Pt 4), 835–844, doi:10.1099/13500872-145-4-835 (1999).

23 Munguia, J. *et al.* The Mla pathway is critical for *Pseudomonas aeruginosa* resistance to outer membrane permeabilization and host innate immune clearance. *Journal of molecular medicine* **95**, 1127–1136, doi:10.1007/s00109-017-1579-4 (2017).

24 Russell, A. B. *et al.* Diverse type VI secretion phospholipases are functionally plastic antibacterial effectors. *Nature* **496**, 508–512, doi:10.1038/nature12074 (2013).

25 Salomon, D. *et al.* Marker for type VI secretion system effectors. *Proc Natl Acad Sci U S A* **111**, 9271–9276, doi:10.1073/pnas.1406110111 (2014).

26 Russell, A. B. *et al.* A widespread bacterial type VI secretion effector superfamily identified using a heuristic approach. *Cell Host Microbe* **11**, 538–549, doi:10.1016/j.chom.2012.04.007 (2012).

27 Gebhardt, M. J., Kambara, T. K., Ramsey, K. M. & Dove, S. L. Widespread targeting of nascent transcripts by RsmA in *Pseudomonas aeruginosa*. *Proc Natl Acad Sci U S A* **117**, 10520–10529, doi:10.1073/pnas.1917587117 (2020).

28 Wilhelm, S., Tommassen, J. & Jaeger, K. E. A novel lipolytic enzyme located in the outer membrane of *Pseudomonas aeruginosa*. *J Bacteriol* **181**, 6977-6986, doi:10.1128/JB.181.22.6977-6986.1999 (1999).

29 Filkin, S. Y., Lipkin, A. V. & Fedorov, A. N. Phospholipase Superfamily: Structure, Functions, and Biotechnological Applications. *Biochemistry (Mosc)* **85**, S177-S195, doi:10.1134/S0006297920140096 (2020).

30 Hernandez, R. E., Gallegos-Monterrosa, R. & Coulthurst, S. J. Type VI secretion system effector proteins: Effective weapons for bacterial competitiveness. *Cell Microbiol* **22**, e13241, doi:10.1111/cmi.13241 (2020).

31 Fridman, C. M., Keppel, K., Gerlic, M., Bosis, E. & Salomon, D. A comparative genomics methodology reveals a widespread family of membrane-disrupting T6SS effectors. *Nat Commun* **11**, 1085, doi:10.1038/s41467-020-14951-4 (2020).

32 Zheng, L., Lin, Y., Lu, S., Zhang, J. & Bogdanov, M. Biogenesis, transport and remodeling of lysophospholipids in Gram-negative bacteria. *Biochim Biophys Acta Mol Cell Biol Lipids* **1862**, 1404-1413, doi:10.1016/j.bbalip.2016.11.015 (2017).

33 Lin, Y. *et al.* The phospholipid-repair system LpIT/Aas in Gram-negative bacteria protects the bacterial membrane envelope from host phospholipase A2 attack. *J Biol Chem* **293**, 3386-3398, doi:10.1074/jbc.RA117.001231 (2018).

34 Morehouse, B. R. *et al.* STING cyclic dinucleotide sensing originated in bacteria. *Nature* **586**, 429-433, doi:10.1038/s41586-020-2719-5 (2020).

35 Flores-Diaz, M., Monturiol-Gross, L., Naylor, C., Alape-Giron, A. & Flieger, A. Bacterial Sphingomyelinases and Phospholipases as Virulence Factors. *Microbiol Mol Biol Rev* **80**, 597-628, doi:10.1128/MMBR.00082-15 (2016).

36 Stover, C. K. *et al.* Complete genome sequence of *Pseudomonas aeruginosa* PA01, an opportunistic pathogen. *Nature* **406**, 959–964 (2000).

37 Yu, Y. *et al.* Genomic patterns of pathogen evolution revealed by comparison of *Burkholderia pseudomallei*, the causative agent of melioidosis, to avirulent *Burkholderia thailandensis*. *BMC microbiology* **6**, 46 (2006).

38 Paulsen, I. T. *et al.* Complete genome sequence of the plant commensal *Pseudomonas fluorescens* Pf-5. *Nat Biotechnol* **23**, 873–878, doi:nbt1110 [pii] 10.1038/nbt1110 (2005).

39 Rietsch, A., Vallet-Gely, I., Dove, S. L. & Mekalanos, J. J. ExsE, a secreted regulator of type III secretion genes in *Pseudomonas aeruginosa*. *Proc Natl Acad Sci U S A* **102**, 8006–8011 (2005).

40 Chandler, J. R. *et al.* Mutational analysis of *Burkholderia thailandensis* quorum sensing and self-aggregation. *J Bacteriol* **191**, 5901–5909 (2009).

41 Gibson, D. G. *et al.* Enzymatic assembly of DNA molecules up to several hundred kilobases. *Nature methods* **6**, 343–345, doi:10.1038/nmeth.1318 (2009).

42 Hoang, T. T., Kutchma, A. J., Becher, A. & Schweizer, H. P. Integration-proficient plasmids for *Pseudomonas aeruginosa*: site-specific integration and use for engineering of reporter and expression strains. *Plasmid* **43**, 59–72 (2000).

43 Leroux, M. *et al.* Quantitative single-cell characterization of bacterial interactions reveals type VI secretion is a double-edged sword. *Proc Natl Acad Sci U S A* **109**, 19804–19809, doi:10.1073/pnas.1213963109 (2012).

44 Choi, K. H. *et al.* Genetic tools for select-agent-compliant manipulation of *Burkholderia pseudomallei*. *Applied and environmental microbiology* **74**, 1064–1075 (2008).

45 Bligh, E. G. & Dyer, W. J. A rapid method of total lipid extraction and purification. *Can J Biochem Physiol* **37**, 911-917, doi:10.1139/o59-099 (1959).

46 Shiva, S. *et al.* Lipidomic analysis of plant membrane lipids by direct infusion tandem mass spectrometry. *Methods in molecular biology (Clifton, N.J)* **1009**, 79-91, doi:10.1007/978-1-62703-401-2_9 (2013).

47 Lee, K. M. *et al.* A Genetic Screen Reveals Novel Targets to Render *Pseudomonas aeruginosa* Sensitive to Lysozyme and Cell Wall-Targeting Antibiotics. *Front Cell Infect Microbiol* **7**, 59, doi:10.3389/fcimb.2017.00059 (2017).

48 Kulasekara, H. D. *et al.* A novel two-component system controls the expression of *Pseudomonas aeruginosa* fimbrial cup genes. *Molecular microbiology* **55**, 368-380, doi:10.1111/j.1365-2958.2004.04402.x (2005).

49 Gallagher, L. A. Methods for Tn-Seq Analysis in *Acinetobacter baumannii*. *Methods in molecular biology (Clifton, N.J)* **1946**, 115-134, doi:10.1007/978-1-4939-9118-1_12 (2019).

50 Chen, I. A. *et al.* The IMG/M data management and analysis system v.6.0: new tools and advanced capabilities. *Nucleic Acids Res* **49**, D751-D763, doi:10.1093/nar/gkaa939 (2021).

51 Dobson, L., Remenyi, I. & Tusnady, G. E. CCTOP: a Consensus Constrained TOPology prediction web server. *Nucleic Acids Res* **43**, W408-412, doi:10.1093/nar/gkv451 (2015).

52 Lopalco, P., Stahl, J., Annese, C., Averhoff, B. & Corcelli, A. Identification of unique cardiolipin and monolysocardiolipin species in *Acinetobacter baumannii*. *Sci Rep* **7**, 2972, doi:10.1038/s41598-017-03214-w (2017).

53 Harvat, E. M. *et al.* Lysophospholipid flipping across the *Escherichia coli* inner membrane catalyzed by a transporter (LpIT) belonging to the major facilitator superfamily. *J Biol Chem* **280**, 12028–12034, doi:10.1074/jbc.M414368200 (2005).

54 Lin, Y., Zheng, L. & Bogdanov, M. Measurement of Lysophospholipid Transport Across the Membrane Using *Escherichia coli* Spheroplasts. *Methods in molecular biology* (Clifton, N.J) **1949**, 165–180, doi:10.1007/978-1-4939-9136-5_13 (2019).

55 Silverman, J. M. *et al.* Separate inputs modulate phosphorylation-dependent and -independent type VI secretion activation. *Molecular microbiology* **82**, 1277–1290, doi:10.1111/j.1365-2958.2011.07889.x (2011).

56 Mougous, J. D. *et al.* A virulence locus of *Pseudomonas aeruginosa* encodes a protein secretion apparatus. *Science* **312**, 1526–1530 (2006).

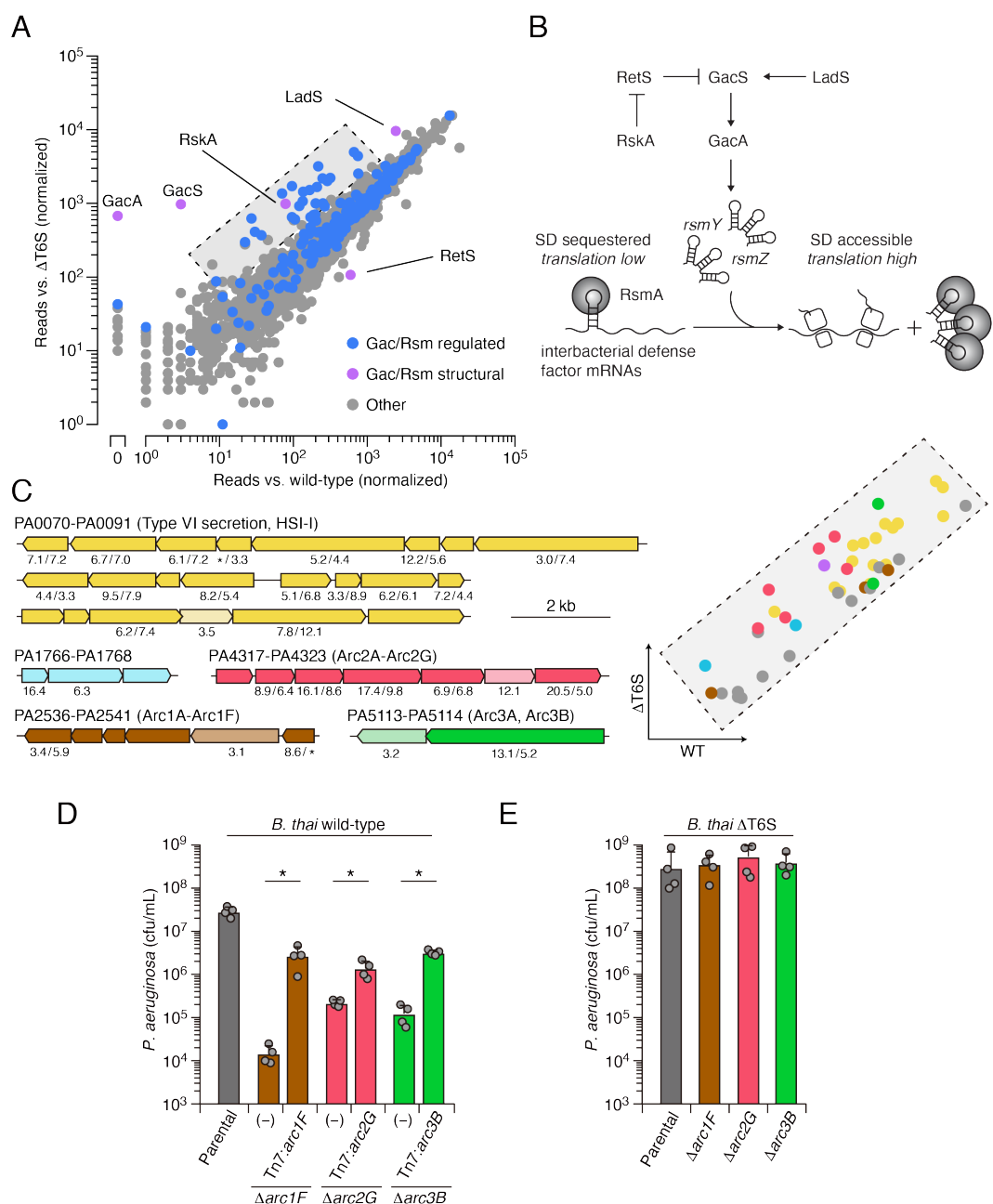


Fig. 1. Multiple pathways under Gac/Rsm control contribute to *P. aeruginosa* defense against antagonism. (A) Transposon library sequencing-based comparison of the fitness contribution of individual *P. aeruginosa* genes during growth competition with wild-type *B. thai* versus *B. thai* $\Delta T6S$. Genes under Gac/Rsm control (blue) and those encoding core Gac/Rsm regulatory factors (purple, labeled) are indicated. (B) Overview of the Gac/Rsm pathway (SD, Shine–Dalgarno). The *rsmY* and *rsmZ* genes encode small RNA molecules that sequester the translational regulator RsmA. (C) Left, *P. aeruginosa* gene clusters hit (>three-fold in replicate screens; Supplemental Table 1) in this study. Numbers below genes indicate transposon insertion ratio (*B. thai* $\Delta T6S$ /wild-type) for screen in A followed by the replicate screen (Supplemental Fig. 1B); light toned genes were hit in only one replicate. Asterisk indicate genes for which insertion were undetected in libraries obtained from *B. thai* wild-type competition. Right, Zoom-in of boxed region of A with genes colored corresponding to clusters at left. (D,E) Recovery of *P. aeruginosa* cells with the indicated genotypes following growth competition against *B. thai* wild-type (D) or $\Delta T6S$ (E).

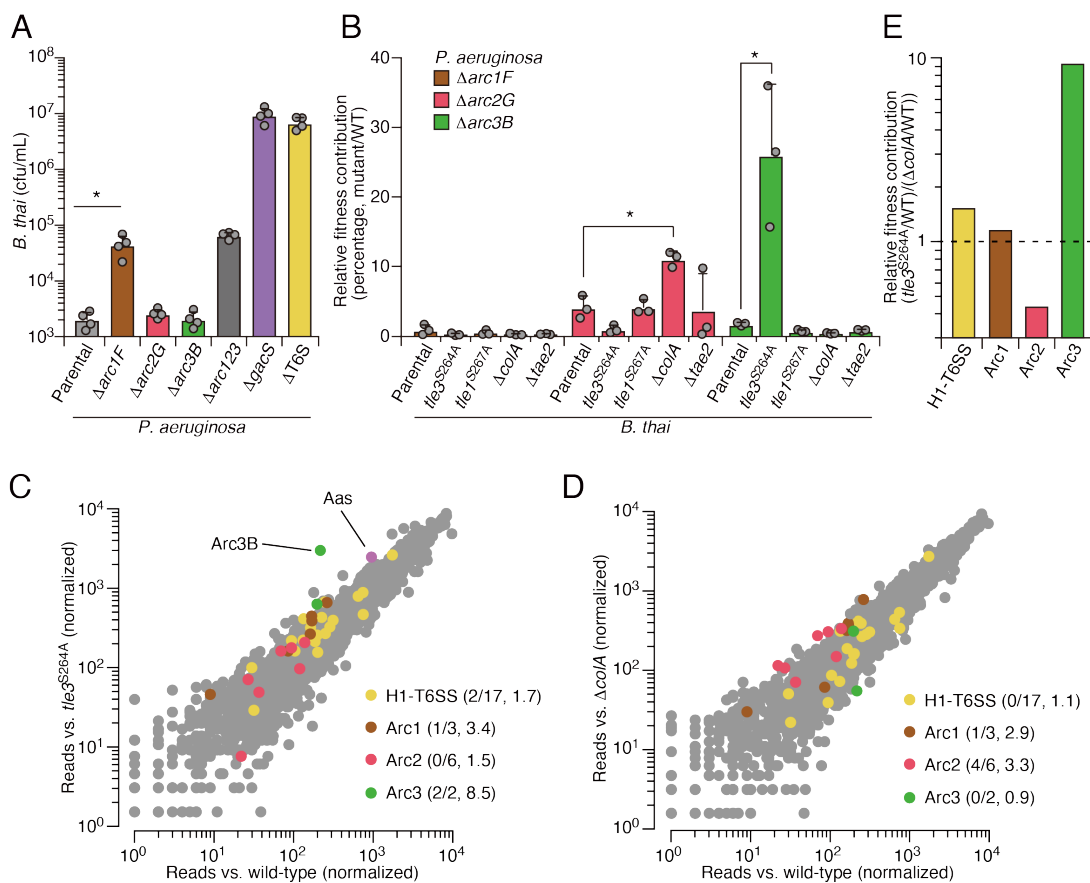


Fig. 2. Arc pathways can provide toxin-specific antagonism defense that eclipses that of other cellular factors. (A) Recovery of *B. thai* cells following growth competition against a relative abundance of *P. aeruginosa* containing the indicated gene deletions, colored according to Fig. 1C. (B) Relative survival of *P. aeruginosa* wild-type versus Arc1-3-inactivated mutants following growth competition against the indicated *B. thai* strains. The loss of ColA or Tle3 activity in *B. thai* increase the relative survival of *P. aeruginosa* lacking Arc2 or Arc3 activity, respectively. (C,D) Transposon library sequencing-based comparison of the fitness contribution of individual *P. aeruginosa* genes during growth competition with wild-type *B. thai* versus *B. thai* lacking Tle3 (C) or ColA (D) activity, colored according to Fig. 1C. Values in parentheses correspond to the number of genes hit (>three-fold change in transposon insertion frequency) within each cluster compared to the number within each cluster hit in the initial screens (*B. thai* wild-type versus *B. thai* Δ T6S) followed by the average transposon insertion frequency ratio (*B. thai* mutant/*B. thai* wild-type) of the genes in the depicted screen. (E) Fitness contribution of each *P. aeruginosa* Arc pathway and the H1-T6SS to defense against Tle3 versus ColA.

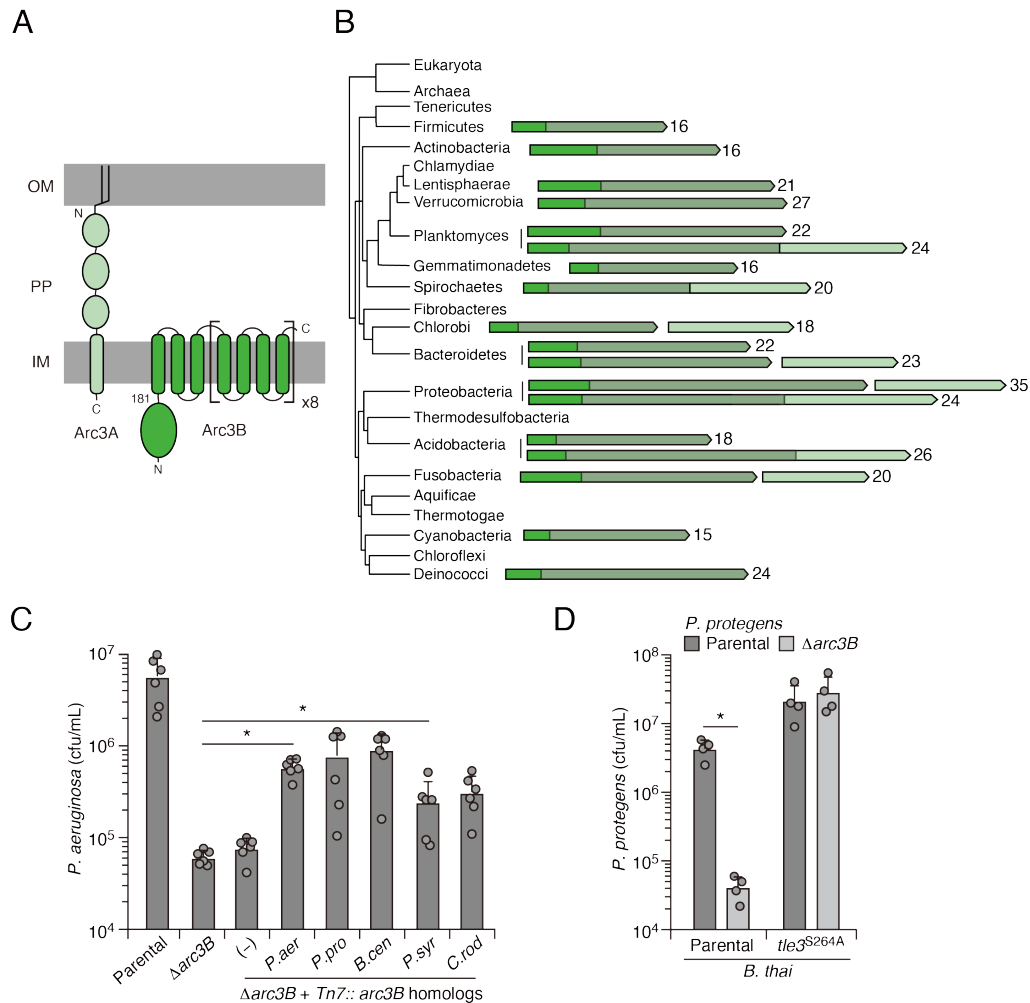


Fig. 3. Arc3B is a predicted massive polytopic membrane protein with functionally complementing family members that occur widely in Gram-negative and -positive bacterial phyla. (A) Schematic depiction of Arc3A and Arc3B based on bioinformatic predictions. **(B)** Phylogeny of bacterial phyla with representative *arc* genes depicted and colored as in A. Membrane associated regions (greyed) and the number of predicted transmembrane segments are indicated. **(C)** Recovery of *P. aeruginosa* strains bearing the indicated mutations and containing a control chromosomal insertion (−) or insertion constructs expressing Arc3B proteins derived from assorted bacteria (*P. aer*, *P. aeruginosa*; *P. pro*, *P. protegens*; *B. cen*, *B. cenocepacia*; *P. syr*, *P. syringae*; *C. rod*, *Citrobacter rodentium*) following growth competition against *B. thai* wild-type. **(D)** Recovery of the indicated *P. protegens* strains following growth competition against *B. thai* wild-type or a strain lacking Tle3 activity.

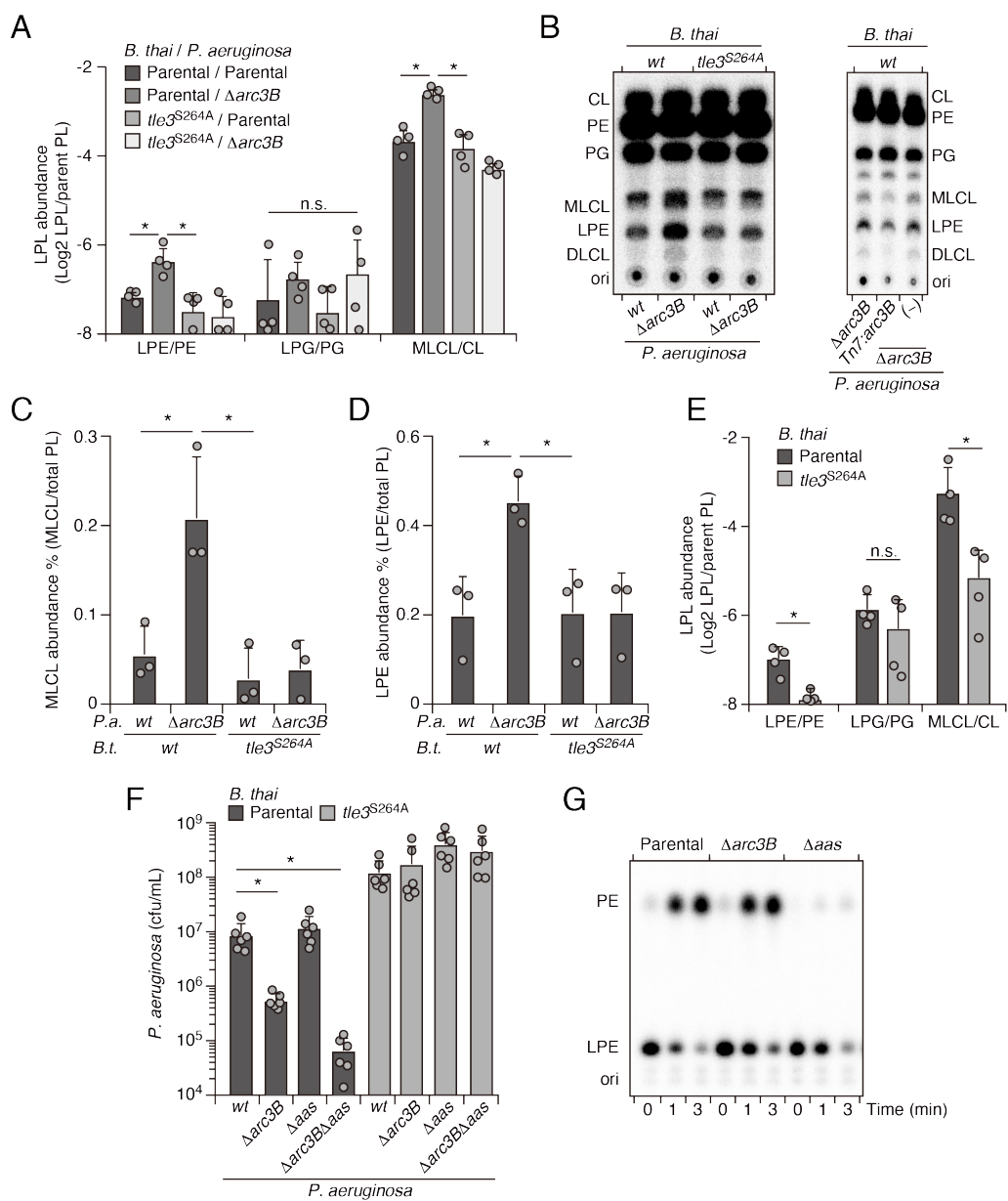
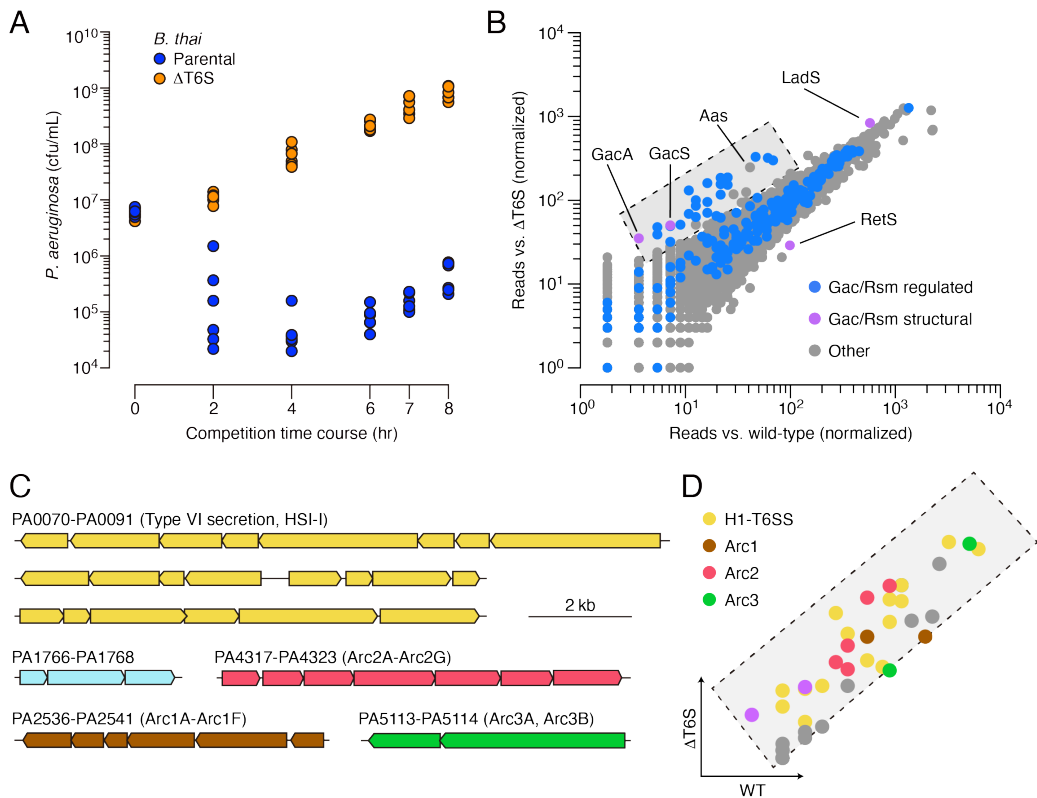
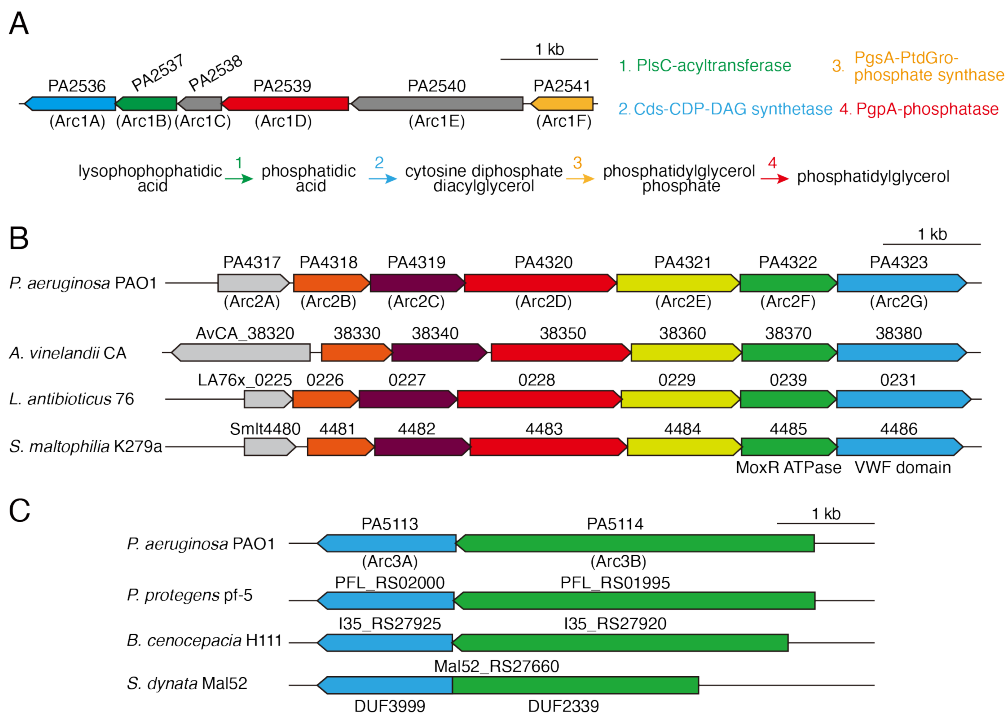


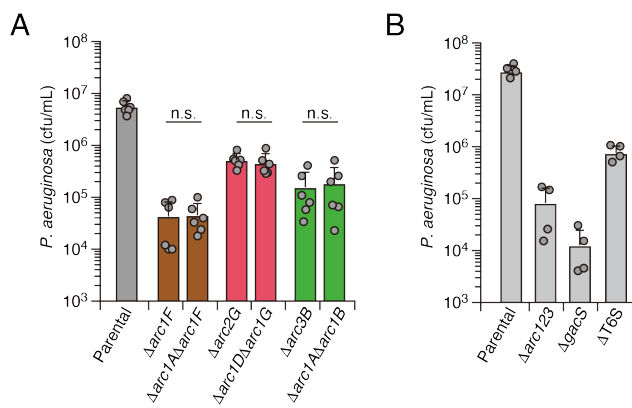
Fig. 4. Arc3 prohibits Tle3-catalyzed lysophospholipid accumulation by a mechanism distinct from known pathways. (A-D) Mass spectrometric (A) and radiographic TLC (B) analysis of major phospholipid and lysophospholipid species within lipid extracts derived from the indicated mixtures of *P. aeruginosa* and *B. thai* strains. *P. aeruginosa* were grown in $^{32}\text{PO}_4^{2-}$ prior to incubation with *B. thai*. Strains were allowed to interact for 1 hr before phospholipids were harvested. Radiolabeled molecules of interest within biological triplicate experiments resolved by TLC were quantified by densitometry (C,D) (E) Mass spectrometric analysis of major phospholipid and lysophospholipid species within lipid extracts derived from mixtures containing *B. thai* lacking Tle3-specific immunity factors competing with the indicated *B. thai* strains. (F) Recovery of the indicated *P. aeruginosa* strains following growth competition against *B. thai* wild-type or a strain lacking Tle3 activity. (G) Radiographic TLC analysis of products extracted after incubation of *P. aeruginosa*-derived spheroplasts purified radiolabeled LPE.



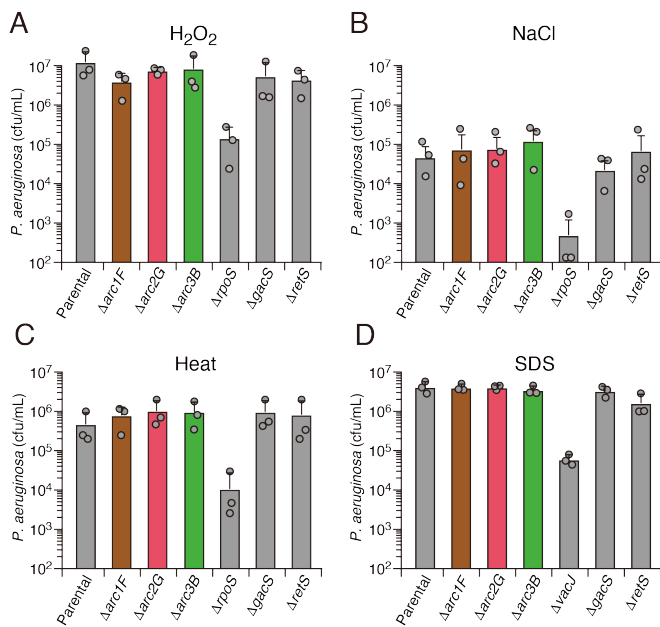
Supplemental Fig. 1. Multiple pathways under Gac/Rsm control contribute to *P. aeruginosa* defense against antagonism. (A) Growth of wild-type *P. aeruginosa* in co-culture with the indicated *B. thai* strains. (B) Transposon library sequencing-based comparison of the fitness contribution of individual *P. aeruginosa* genes during growth competition with wild-type *B. thai* versus *B. thai* Δ T6S. Genes under Gac/Rsm control (blue) and those encoding core Gac/Rsm regulatory factors (purple, labeled) are indicated. This experiment is a biological replicate of that in Fig. 1A. (C) *P. aeruginosa* gene clusters hit (Supplemental Table 1) in this study. (D) Zoom-in of boxed region of B with genes colored corresponding to clusters at left.



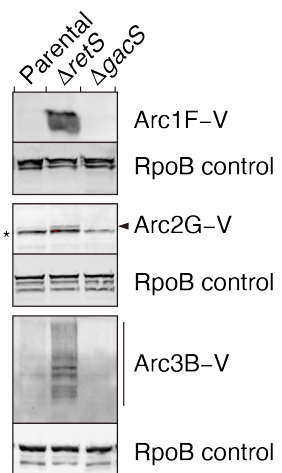
Supplemental Fig. 2. Antagonism resistance clusters possess functionally related genes and are in diverse bacteria. (A) Schematic depicting the *arc1* gene cluster of *P. aeruginosa*. Predicted enzymatic activity of Arc1A, B, D, F are indicated (right) and placed onto a phospholipid biosynthesis pathway (bottom). (B) Depiction of *arc2* genes from the indicated species. Genes encoding the predicted MoxR-like ATPase and Von Willebrand Factor (VWF) domain protein are indicated below the respective genes. Orthologs are colored to highlight synteny. (C) Depiction of *arc2* genes from the indicated species. *S. dynata* exemplifies an instance of translational fusion of *arc3A,B*. Domains of unknown function constituting the two proteins are indicated below.



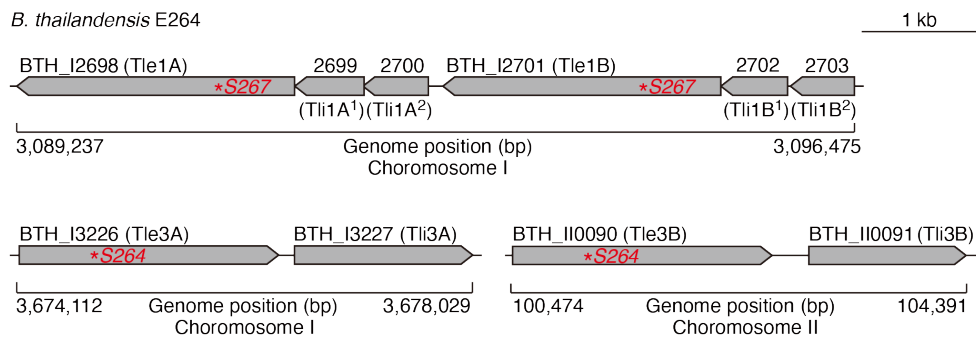
Supplemental Fig. 3. Interbacterial competition assays measure the contribution of *arc1-3* to *P. aeruginosa* fitness during antagonism by *B. thai*. (A) Recovery of *P. aeruginosa* strains bearing the indicated single or double deletions within *arc1-3* following growth competition against wild-type *B. thai*. (B) Recovery of *P. aeruginosa* cells with the indicated genotypes following growth competition against wild-type *B. thai*.



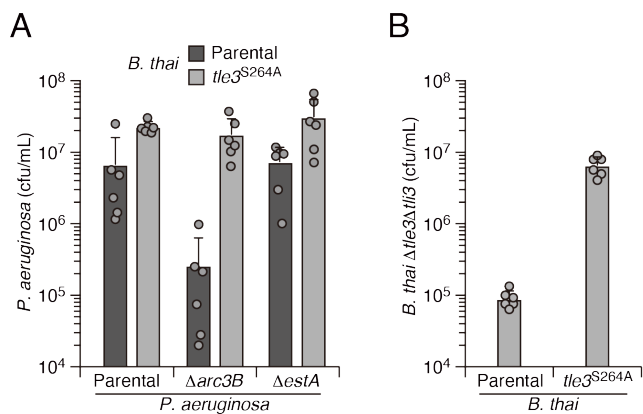
Supplemental Fig. 4. Arc1-3 do not contribute to the survival of *P. aeruginosa* exposed to common environmental stresses. Survival of the indicated *P. aeruginosa* strains during exposure to hydrogen peroxide (50 mM, 30 min) (A), high salinity (3M NaCl, 20 hours) (B), high temperature (55°C, 30 min) (C), or detergent (0.5% (w/v) SDS) (D).



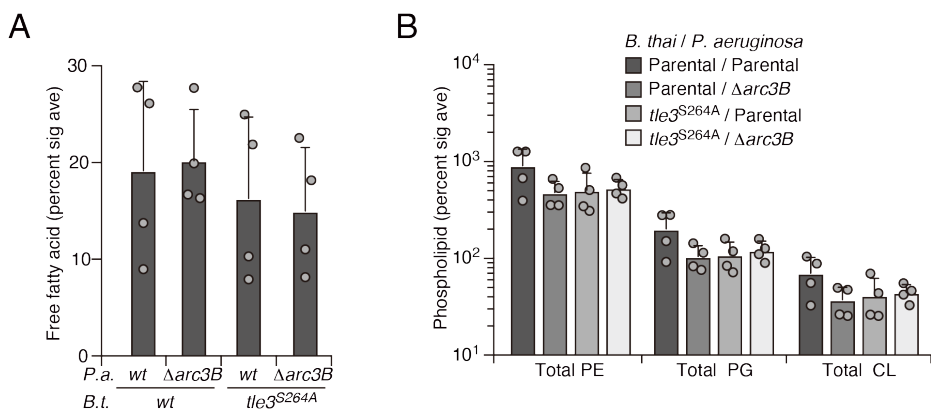
Supplemental Fig. 5. Arc1-3 are subject to tight regulation by the Gac/Rsm signaling pathway.
Anti-VSV-G immunoblot analysis was used to probe levels of the indicated VSV-G-tagged (-V) Arc proteins encoded at their respective native genomic loci in *P. aeruginosa* wild-type, $\Delta retS$, or $\Delta gacS$ backgrounds. The asterisk denotes a non-specific VSV-G antibody-reactive band. The arrow highlights the position of Arc2G-V.



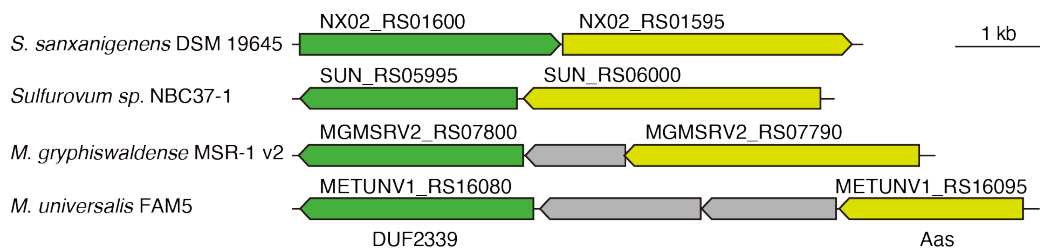
Supplemental Fig. 6. The loci encoding Tle1 and Tle3 are duplicated in *B. thai*. Schematic depicting the *tle1/tli1* (top) *tle3/tli3* (bottom) loci in the genome *B. thai* E264 strain. Predicted catalytic serine residues mutagenized in this study are indicated by red asterisks.



Supplemental Fig. 7. EstA is not involved in defense against Tle3 and Tle3 induces potent self-intoxication within *B. thai*. (A) Recovery of the indicated *P. aeruginosa* strains following growth competition against *B. thai* wild-type or a strain lacking Tle3 activity. (B) Recovery of *B. thai* strain sensitized to Tle3 intoxication ($\Delta tle3\Delta tl3$) following growth competition against *B. thai* wild-type or a strain lacking Tle3 activity.



Supplemental Fig. 8. Tle3 intoxication does not impact free fatty acids nor intact parent phospholipids in *P. aeruginosa*. Mass spectrometric analysis of free fatty acid (A) and parent phospholipid species (B) within lipid extracts derived from the indicated mixtures.



Supplemental Fig. 9. *Arc3B* genes are encoded adjacent to *aas* genes in diverse bacteria. Schematic depicting *arc3B* and *aas* loci in the indicated bacterial species.

Supplemental Table 1. Transposon sequencing-based analysis of *P. aeruginosa* fitness determinants during antagonism by *B. thai*.

Replicate 1		Normalized insertion counts ¹			
Locus ID ²	Gene name	TA sites	+ <i>B.t.</i> WT	+ <i>B.t.</i> ΔT6S	Fold change (ΔT6S/WT)
Genes with higher insertion frequency + <i>B.t.</i> ΔT6S					
PA0005	lptA	11	2.26180694	7	3.094870688
PA0011	PA0011	22	115.352154	197	1.707813796
PA0066	PA0066	3	382.245374	651	1.703094515
PA0070	PA0070	16	236.358826	1681	7.112067818
PA0071	PA0071	27	743.003581	4973	6.693103677
PA0072	PA0072	9	107.43583	656	6.10597042
PA0073	PA0073	4	0	43	N.D. ³
PA0074	ppkA	29	848.177604	4410	5.199382746
PA0075	pppA	8	33.9271042	414	12.20263296
PA0077	icmF1	30	853.832121	2554	2.991220331
PA0078	PA0078	10	225.049791	1000	4.443461136
PA0079	PA0079	15	152.671969	1454	9.523686696
PA0081	fha1	6	186.599073	1526	8.177961313
PA0082	PA0082	10	118.744865	611	5.14548566
PA0083	PA0083	5	211.478949	700	3.310022124
PA0084	PA0084	18	357.365497	2221	6.214925668
PA0085	hcp1	5	150.410162	1082	7.193662886
PA0087	PA0087	1	229.573405	588	2.561272287
PA0088	PA0088	20	326.831103	2040	6.241756006
PA0089	PA0089	15	286.118578	1011	3.533500016
PA0090	clpV1	15	280.464061	2196	7.829880207
PA0120	PA0120	3	97.2576986	77	0.791711105
PA0125	PA0125	2	45.2361389	33	0.729505232

PA0171	PA0171	10	1.13090347	21	18.56922413
PA0180	cttP	5	3.39271042	61	17.9797249
PA0197	tonB2	2	5.65451736	26	4.598093585
PA0278	PA0278	4	110.82854	47	0.424078491
PA0374	ftsE	6	62.199691	213	3.424454311
PA0401	PA0401	9	3.39271042	12	3.536995061
PA0407	gshB	10	7.9163243	35	4.421243834
PA0409	pilH	3	365.281821	1121	3.068863369
PA0424	mexR	2	251.060571	960	3.823778446
PA0512	PA0512	5	32.7962007	48	1.463584164
PA0667	PA0667	30	148.148355	508	3.428995212
PA0674	vreA	7	203.562625	210	1.031623561
PA0680	PA0680	3	89.3413743	68	0.76112552
PA0712	PA0712	4	7.9163243	40	5.052850096
PA0714.1	phrD	4	29.4034903	41	1.394392284
PA0715	PA0715	61	15.8326486	5	0.315803131
PA0753	PA0753	5	16.9635521	82	4.83389325
PA0762	algU	13	87.0795673	177	2.032623789
PA0764	mucB	5	49.7597528	125	2.512070357
PA0766	mucD	11	114.221251	592	5.182923447
PA0819	PA0819	2	127.792092	102	0.798171455
PA0928	gacS	18	3.39271042	985	290.3283446
PA0951a	PA0951a	1	6.78542083	22	3.242245478
PA0967	rvvB	17	7.9163243	54	6.82134763
PA0973	oprL	11	16.9635521	90	5.305492592
PA1034	PA1034	2	6.78542083	73	10.75835999
PA1045	PA1045	17	6.78542083	21	3.094870683
PA1103	PA1103	2	0	38	N.D.
PA1151	imm2	16	1.13090347	4	3.536995072

PA1233	PA1233	5	18.0944556	80	4.42124382
PA1235	PA1235	7	81.42505	105	1.289529451
PA1263	PA1263	8	185.468169	215	1.159228568
PA1276	cobC	7	123.268478	193	1.565688188
PA1281	cobV	5	59.937884	98	1.635026021
PA1285	PA1285	6	13.5708417	44	3.242245468
PA1294	rnd	13	10.1781312	43	4.224744126
PA1298	PA1298	0	142.493837	194	1.361462391
PA1394	PA1394	0	12.4399382	54	4.340857578
PA1404	PA1404	2	45.2361389	178	3.934907009
PA1447	fliQ	1	24.8798764	87	3.496801937
PA1503	PA1503	4	88.2104708	45	0.510143519
PA1553	ccoO1	11	10.1781312	38	3.733494809
PA1611	PA1611	23	88.2104708	995	11.27984003
PA1615	PA1615	5	12.4399382	87	6.993603875
PA1629	PA1629	5	23.7489729	81	3.410673815
PA1632	kdpF	3	2.26180694	14	6.189741376
PA1652	PA1652	11	133.44661	146	1.094070505
PA1656	PA1656	11	98.3886021	305	3.099952571
PA1696	pscO	3	5.65451736	47	8.311938404
PA1697	PA1697	13	53.1524632	87	1.636800907
PA1707	pcrH	9	184.337266	193	1.046993938
PA1709	popD	1	156.064679	91	0.583091578
PA1710	exsC	2	221.657081	79	0.35640639
PA1747	PA1747	1	0	10	N.D.
PA1766	PA1766	13	9.04722778	148	16.35860217
PA1767	PA1767	15	50.8906562	319	6.26834126
PA1776	sigX	12	22.6180694	25	1.10531096
PA1801	clpP	12	24.8798764	20	0.803862514

PA1879	PA1879	2	2.26180694	10	4.42124384
PA1957	PA1957	5	66.7233048	87	1.30389225
PA2010	PA2010	6	62.199691	99	1.591647778
PA2051	PA2051	7	111.959444	113	1.009294044
PA2088	PA2088	6	109.697637	100	0.911596665
PA2132	cupA5	9	213.740756	191	0.893605897
PA2143	PA2143	2	99.5195055	83	0.834007359
PA2146	PA2146	1	0	21	N.D.
PA2159	PA2159	2	1.13090347	16	14.14798029
PA2193	hcnA	2	1.13090347	19	16.80072659
PA2236	pslF	9	82.5559535	79	0.956926747
PA2241	pslK	10	2.26180694	21	9.284612063
PA2242	pslL	13	21.487166	83	3.862770921
PA2259	ptxS	9	160.588293	201	1.251647902
PA2279	arsC	3	19.225359	70	3.641024337
PA2284	PA2284	5	40.712525	122	2.996620819
PA2297	PA2297	3	19.225359	78	4.057141404
PA2321	PA2321	3	1.13090347	16	14.14798029
PA2330	PA2330	3	2.26180694	18	7.958238911
PA2449	PA2449	10	218.26437	261	1.195797555
PA2536	PA2536	11	192.25359	657	3.417361413
PA2540	PA2540	19	298.558517	915	3.064725834
PA2541	PA2541	5	10.1781312	88	8.645987979
PA2558	PA2558	4	84.8177604	94	1.108258454
PA2570	lecA	14	114.221251	112	0.980553085
PA2577	PA2577	5	2.26180694	10	4.42124384
PA2586	gacA	11	0	685	N.D.
PA2659	PA2659	5	0	27	N.D.
PA2724	PA2724	4	46.3670424	141	3.040953071

PA2743	infC	12	2.26180694	7	3.094870688
PA2830	htpX	4	74.6396292	124	1.661315863
PA2853	oprI	3	163.981003	180	1.097688127
PA2882	PA2882	7	57.6760771	26	0.450793489
PA2913	PA2913	11	84.8177604	106	1.249738256
PA2946	PA2946	5	80.2941465	103	1.282783422
PA2963	PA2963	17	960.137048	2075	2.161149811
PA2992	PA2992	2	28.2725868	91	3.21866551
PA3033	PA3033	1	28.2725868	85	3.006445806
PA3051	PA3051	2	5.65451736	50	8.842487664
PA3080	PA3080	7	122.137575	222	1.817622464
PA3094.2	PA3094.2	3	2.26180694	10	4.42124384
PA3110	PA3110	3	105.174023	107	1.017361483
PA3111	folC	15	5.65451736	30	5.305492598
PA3142	PA3142	5	127.792092	160	1.252033655
PA3145	wbpL	34	1.13090347	5	4.42124384
PA3173	PA3173	11	12.4399382	48	3.858540069
PA3205	PA3205	1	5.65451736	23	4.067544325
PA3209	PA3209	7	106.304926	85	0.799586653
PA3214	PA3214	9	153.802872	149	0.968772547
PA3224	PA3224	3	228.442501	81	0.354575001
PA3265	PA3265	3	93.8649882	150	1.598039939
PA3267	PA3267	22	1083.40553	2305	2.127550521
PA3288	PA3288	3	10.1781312	38	3.733494809
PA3298	PA3298	1	38.450718	64	1.664468268
PA3299	fadD1	19	24.8798764	280	11.2540752
PA3317	PA3317	8	211.478949	647	3.059406163
PA3385	amrZ	3	22.6180694	82	3.625419949
PA3432	PA3432	3	62.199691	49	0.787785264

PA3439	folX	3	67.8542083	128	1.886397369
PA3574	nalD	6	54.2833667	179	3.297511022
PA3574a	PA3574a	3	12.4399382	57	4.582016332
PA3576	PA3576	5	148.148355	235	1.586247785
PA3596	PA3596	8	188.86088	170	0.900133474
PA3616	PA3616	5	61.0687875	81	1.326373149
PA3634	PA3634	2	4.52361389	36	7.958238894
PA3646	lpxD	16	11.3090347	34	3.006445811
PA3649	PA3649	20	24.8798764	98	3.93892632
PA3675	PA3675	4	363.020015	438	1.206545044
PA3738	xerD	9	10.1781312	33	3.242245492
PA3767	PA3767	6	67.8542083	75	1.105310958
PA3778	PA3778	6	33.9271042	57	1.680072654
PA3888	PA3888	6	222.787984	198	0.888737339
PA3974	ladS	36	2758.27357	9680	3.509441596
PA4020	mpl	15	1.13090347	15	13.26373152
PA4045	PA4045	6	66.7233048	93	1.393815853
PA4110	ampC	21	1177.27051	1454	1.235060241
PA4269	rpoC	49	29.4034903	60	2.040574074
PA4275	nusG	9	9.04722778	38	4.200181638
PA4277	tufB	23	2.26180694	13	5.747616992
PA4318	PA4318	7	41.8434285	371	8.866386271
PA4319	PA4319	13	107.43583	1727	16.07471176
PA4320	PA4320	19	79.163243	1374	17.35654008
PA4321	PA4321	17	135.708417	934	6.88240288
PA4322	PA4322	6	24.8798764	301	12.09813084
PA4323	PA4323	15	30.5343937	627	20.53422138
PA4351	PA4351	4	10.1781312	59	5.79674194
PA4413	ftsW	12	10.1781312	30	2.947495902

PA4417	murE	16	58.8069805	34	0.578162655
PA4422	PA4422	6	0	16	N.D.
PA4423	PA4423	18	41.8434285	127	3.035124141
PA4424	PA4424	5	67.8542083	114	1.680072657
PA4428	sspA	12	184.337266	212	1.15006588
PA4431	PA4431	8	2.26180694	7	3.094870688
PA4451	PA4451	2	5.65451736	20	3.536995065
PA4610	PA4610	1	19.225359	69	3.589009703
PA4634	PA4634	8	0	2	N.D.
PA4664	hemK	11	0	14	N.D.
PA4671	PA4671	7	2.26180694	11	4.863368224
PA4726.1	PA4726.1	4	1.13090347	18	15.91647782
PA4729	panB	5	1.13090347	14	12.37948275
PA4793	PA4793	9	158.326486	224	1.414798027
PA4795	PA4795	0	49.7597528	98	1.96946316
PA4853	fis	4	1.13090347	13	11.49523398
PA4890	desT	2	0	25	N.D.
PA4932	rplI	4	11.3090347	10	0.884248768
PA4952	PA4952	5	4.52361389	15	3.315932872
PA4960	PA4960	11	36.1889111	59	1.630333663
PA5000	wapR	21	6.78542083	25	3.684369861
PA5005	PA5005	32	10.1781312	17	1.670247678
PA5016	aceF	7	3.39271042	20	5.894991769
PA5049	rpmE	7	4.52361389	17	3.758057255
PA5060	phaF	4	176.420942	129	0.731205709
PA5113	PA5113	15	223.918887	707	3.157393329
PA5114	PA5114	37	246.536957	3226	13.08525926
PA5162	rmlD	11	6.78542083	53	7.810864105
PA5239	rho	10	57.6760771	161	2.791451987

PA5241	ppx	15	11.3090347	35	3.094870688
PA5259	hemD	13	27.1416833	121	4.458087535
PA5280	sss	8	5.65451736	17	3.006445806
PA5285	PA5285	1	9.04722778	79	8.731956564
PA5366	pstB	11	1.13090347	9	7.958238911
PA5405	PA5405	3	105.174023	59	0.560975023
PA5409	PA5409	2	36.1889111	32	0.884248766
PA5555	atpG	15	1.13090347	6	5.305492608

<i>Genes with higher insertion frequency + B.t. WT</i>					
PA0285	PA0285	25	3788.52663	975	0.257355984
PA0427	oprM	21	27.1416833	7	0.25790589
PA0542	PA0542	0	83.6868569	86	1.027640459
PA0624	PA0624	4	143.624741	117	0.814622879
PA0635	PA0635	4	37.3198146	36	0.964635017
PA0787	PA0787	5	106.304926	148	1.392221467
PA0823	PA0823	0	44.1052354	13	0.294749589
PA0905	rsmA	4	166.24281	42	0.252642505
PA1030.1	PA1030.1	2	62.199691	13	0.209004254
PA1082	flgG	6	1143.34341	559	0.488916974
PA1117	PA1117	1	53.1524632	13	0.244579446
PA1149	PA1149	3	97.2576986	30	0.308458872
PA1159	PA1159	3	36.1889111	11	0.303960513
PA1300	PA1300	2	94.9958916	190	2.000086496
PA1444	fliN	4	220.526177	97	0.439857079
PA1612	PA1612	9	534.917342	153	0.2860255
PA1635	kdpC	7	56.5451736	115	2.033772163
PA1644	PA1644	7	94.9958916	67	0.705293659
PA1692	PA1692	4	45.2361389	13	0.287380849

PA1718	pscE	0	134.577513	91	0.676190234
PA1891	PA1891	4	47.4979458	57	1.200051898
PA2008	fahA	11	196.777204	47	0.238848805
PA2066	PA2066	5	57.6760771	59	1.022954455
PA2145	PA2145	5	59.937884	66	1.101139974
PA2161	PA2161	2	23.7489729	7	0.294749589
PA2198	PA2198	5	228.442501	146	0.639110495
PA2312	PA2312	7	121.006672	94	0.77681667
PA2315	PA2315	10	99.5195055	194	1.949366599
PA2334	PA2334	7	16.9635521	39	2.29904679
PA2351	PA2351	9	122.137575	107	0.876061278
PA2469	PA2469	6	195.646301	208	1.063143024
PA2492	mexT	8	20109.7255	5718	0.284340032
PA2495	oprN	10	107.43583	104	0.968019701
PA2497	PA2497	5	41.8434285	49	1.171032149
PA2614	lolA	5	71.2469187	7	0.098249863
PA2970	rpmF	5	33.9271042	7	0.206324712
PA3017	PA3017	3	58.8069805	54	0.918258335
PA3085	PA3085	2	4.52361389	4	0.884248766
PA3139.1	PA3139.1	3	19.225359	3	0.1560439
PA3181	PA3181	5	72.3778222	22	0.303960513
PA3194	edd	9	12.4399382	17	1.366566274
PA3411	PA3411	2	148.148355	39	0.263249632
PA3448	PA3448	8	187.729976	140	0.745751973
PA3480	PA3480	10	30.5343937	25	0.818748859
PA3520	PA3520	4	63.3305944	20	0.315803131
PA3808	PA3808	2	52.0215597	2	0.038445599
PA3813	iscU	3	44.1052354	8	0.181384362
PA3816	cysE	8	144.755644	27	0.186521225

PA3833	PA3833	2	24.8798764	41	1.647918154
PA3844	PA3844	8	1015.55132	316	0.311161035
PA3937	PA3937	4	33.9271042	2	0.058949918
PA4033	PA4033	3	12.4399382	1	0.080386251
PA4092	hpaC	1	42.9743319	6	0.139618226
PA4138	tyrS	10	934.126268	267	0.285828596
PA4479	mreD	6	63.3305944	20	0.315803131
PA4482	gatC	2	29.4034903	4	0.136038272
PA4561	ribF	7	30.5343937	6	0.196499726
PA4637	PA4637	1	91.6031812	29	0.316582892
PA4663	moeB	9	31.6652972	7	0.221062192
PA4732	pgi	24	85.9486639	121	1.407817114
PA4822	PA4822	9	27.1416833	51	1.87902863
PA4856	retS	20	669.494855	108	0.161315653
PA4916	PA4916	5	54.2833667	18	0.331593287
PA4918	PA4918	10	464.801327	100	0.215145685
PA5062	PA5062	0	23.7489729	2	0.084214168
PA5134	PA5134	11	360.758208	187	0.518352724
PA5161	rmlB	19	49.7597528	2	0.040193126
PA5183a	PA5183a	3	102.912216	125	1.214627426
PA5203	gshA	25	1049.47842	383	0.364943188
PA5231	PA5231	27	4334.75301	4400	1.015052066
PA5443	uvrD	22	67.8542083	47	0.692661534

Replicate 2		Normalized insertion counts			
Locus ID	Gene name	TA sites	+ <i>B.t.</i> WT	+ <i>B.t.</i> Δ T6S	Fold change (Δ T6S /WT)
<i>Genes with higher insertion frequency + B.t. ΔT6S</i>					
PA0005	lptA	11	25.2832219	7	0.276863449

PA0011	PA0011	22	5.41783325	20	3.691512652
PA0066	PA0066	3	12.6416109	51	4.034295969
PA0070	PA0070	16	21.671333	156	7.198449671
PA0071	PA0071	27	46.9545549	329	7.006774975
PA0072	PA0072	9	5.41783325	39	7.198449671
PA0073	PA0073	4	1.80594442	6	3.322361386
PA0074	ppkA	29	68.6258879	300	4.37152814
PA0075	pppA	8	9.02972209	51	5.648014357
PA0077	icmF1	30	25.2832219	187	7.396209277
PA0078	PA0078	10	19.8653886	65	3.272022578
PA0079	PA0079	15	12.6416109	100	7.910384253
PA0081	fha1	6	21.671333	117	5.398837253
PA0082	PA0082	10	7.22377767	49	6.783154497
PA0083	PA0083	5	5.41783325	48	8.859630364
PA0084	PA0084	18	25.2832219	153	6.051443954
PA0085	hcp1	5	16.2534998	71	4.368289971
PA0087	PA0087	1	7.22377767	32	4.429815182
PA0088	PA0088	20	25.2832219	188	7.435761198
PA0089	PA0089	15	41.5367216	85	2.046382013
PA0090	clpV1	15	10.8356665	131	12.08970393
PA0120	PA0120	3	1.80594442	7	3.876088284
PA0125	PA0125	2	1.80594442	6	3.322361386
PA0171	PA0171	10	5.41783325	3	0.553726898
PA0180	cttP	5	1.80594442	3	1.661180693
PA0197	tonB2	2	1.80594442	3	1.661180693
PA0278	PA0278	4	1.80594442	7	3.876088284
PA0374	ftsE	6	5.41783325	18	3.322361386
PA0401	PA0401	9	32.5069995	44	1.353554639
PA0407	gshB	10	16.2534998	14	0.861352952

PA0409	pilH	3	50.5664437	89	1.760060496
PA0424	mexR	2	23.4772774	53	2.257501968
PA0512	PA0512	5	1.80594442	7	3.876088284
PA0667	PA0667	30	7.22377767	11	1.522748969
PA0674	vreA	7	5.41783325	18	3.322361386
PA0680	PA0680	3	5.41783325	18	3.322361386
PA0712	PA0712	4	1.80594442	3	1.661180693
PA0714.1	phrD	4	1.80594442	7	3.876088284
PA0715	PA0715	61	1.80594442	14	7.752176568
PA0753	PA0753	5	7.22377767	7	0.969022071
PA0762	algU	13	1.80594442	16	8.859630364
PA0764	mucB	5	1.80594442	6	3.322361386
PA0766	mucD	11	16.2534998	22	1.353554639
PA0819	PA0819	2	5.41783325	17	3.137785754
PA0928	gacS	18	7.22377767	50	6.921586222
PA0951a	PA0951a	1	0.1	2	20
PA0967	ruvB	17	10.8356665	5	0.461439081
PA0973	oprL	11	3.61188884	8	2.214907591
PA1034	PA1034	2	3.61188884	0	0
PA1045	PA1045	17	3.61188884	4	1.107453795
PA1103	PA1103	2	1.80594442	2	1.107453795
PA1151	imm2	16	0	0	N.D.
PA1233	PA1233	5	5.41783325	8	1.476605061
PA1235	PA1235	7	1.80594442	13	7.198449671
PA1263	PA1263	8	5.41783325	20	3.691512652
PA1276	cobC	7	1.80594442	15	8.305903466
PA1281	cobV	5	1.80594442	6	3.322361386
PA1285	PA1285	6	3.61188884	4	1.107453795
PA1294	rnd	13	5.41783325	6	1.107453795

PA1298	PA1298	0	5.41783325	17	3.137785754
PA1394	PA1394	0	1.80594442	4	2.214907591
PA1404	PA1404	2	14.4475553	11	0.761374484
PA1447	fliQ	1	3.61188884	1	0.276863449
PA1503	PA1503	4	1.80594442	11	6.090995875
PA1553	ccoO1	11	3.61188884	9	2.49177104
PA1611	PA1611	23	61.4021102	111	1.80775546
PA1615	PA1615	5	5.41783325	2	0.369151265
PA1629	PA1629	5	16.2534998	6	0.369151265
PA1632	kdpF	3	0	0	N.D.
PA1652	PA1652	11	1.80594442	14	7.752176568
PA1656	PA1656	11	19.8653886	33	1.661180693
PA1696	pscO	3	5.41783325	7	1.292029428
PA1697	PA1697	13	3.61188884	11	3.045497938
PA1707	pcrH	9	5.41783325	22	4.060663917
PA1709	popD	1	1.80594442	8	4.429815182
PA1710	exsC	2	5.41783325	17	3.137785754
PA1747	PA1747	1	1.80594442	2	1.107453795
PA1766	PA1766	13	1.80594442	5	2.768634489
PA1767	PA1767	15	19.8653886	8	0.402710471
PA1776	sigX	12	1.80594442	8	4.429815182
PA1801	clpP	12	3.61188884	11	3.045497938
PA1879	PA1879	2	0	0	N.D.
PA1957	PA1957	5	1.80594442	10	5.537268977
PA2010	PA2010	6	3.61188884	13	3.599224835
PA2051	PA2051	7	3.61188884	13	3.599224835
PA2088	PA2088	6	1.80594442	7	3.876088284
PA2132	cupA5	9	7.22377767	23	3.183929662
PA2143	PA2143	2	1.80594442	7	3.876088284

PA2146	PA2146	1	1.80594442	1	0.553726898
PA2159	PA2159	2	0	0	#DIV/0!
PA2193	hcnA	2	0	0	N.D.
PA2236	pslF	9	3.61188884	14	3.876088284
PA2241	pslK	10	0	0	N.D.
PA2242	pslL	13	1.80594442	1	0.553726898
PA2259	ptxS	9	1.80594442	14	7.752176568
PA2279	arsC	3	0.1	5	50
PA2284	PA2284	5	3.61188884	7	1.938044142
PA2297	PA2297	3	7.22377767	10	1.384317244
PA2321	PA2321	3	0	0	N.D.
PA2330	PA2330	3	0.1	1	10
PA2449	PA2449	10	7.22377767	26	3.599224835
PA2536	PA2536	11	16.2534998	96	5.906420243
PA2540	PA2540	19	48.7604993	107	2.194399187
PA2541	PA2541	5	0.1	16	160
PA2558	PA2558	4	1.80594442	6	3.322361386
PA2570	lecA	14	3.61188884	11	3.045497938
PA2577	PA2577	5	0	0	N.D.
PA2586	gacA	11	3.61188884	35	9.69022071
PA2659	PA2659	5	0.1	2	20
PA2724	PA2724	4	12.6416109	21	1.661180693
PA2743	infC	12	1.80594442	1	0.553726898
PA2830	htpX	4	5.41783325	22	4.060663917
PA2853	oprI	3	9.02972209	30	3.322361386
PA2882	PA2882	7	1.80594442	8	4.429815182
PA2913	PA2913	11	1.80594442	12	6.644722773
PA2946	PA2946	5	3.61188884	12	3.322361386
PA2963	PA2963	17	28.8951107	118	4.083735871

PA2992	PA2992	2	9.02972209	11	1.218199175
PA3033	PA3033	1	7.22377767	5	0.692158622
PA3051	PA3051	2	1.80594442	6	3.322361386
PA3080	PA3080	7	3.61188884	13	3.599224835
PA3094.2	PA3094.2	3	1.80594442	0	0
PA3110	PA3110	3	5.41783325	20	3.691512652
PA3111	folC	15	1.80594442	5	2.768634489
PA3142	PA3142	5	5.41783325	18	3.322361386
PA3145	wbpL	34	0	0	N.D.
PA3173	PA3173	11	1.80594442	2	1.107453795
PA3205	PA3205	1	1.80594442	0	0
PA3209	PA3209	7	7.22377767	28	3.876088284
PA3214	PA3214	9	3.61188884	11	3.045497938
PA3224	PA3224	3	1.80594442	12	6.644722773
PA3265	PA3265	3	3.61188884	11	3.045497938
PA3267	PA3267	22	41.5367216	248	5.970620463
PA3288	PA3288	3	1.80594442	6	3.322361386
PA3298	PA3298	1	1.80594442	8	4.429815182
PA3299	fadD1	19	1.80594442	7	3.876088284
PA3317	PA3317	8	46.9545549	64	1.363020056
PA3385	amrZ	3	3.61188884	5	1.384317244
PA3432	PA3432	3	1.80594442	14	7.752176568
PA3439	folX	3	1.80594442	7	3.876088284
PA3574	nalD	6	1.80594442	14	7.752176568
PA3574a	PA3574a	3	3.61188884	4	1.107453795
PA3576	PA3576	5	7.22377767	24	3.322361386
PA3596	PA3596	8	5.41783325	18	3.322361386
PA3616	PA3616	5	1.80594442	7	3.876088284
PA3634	PA3634	2	0.1	6	60

PA3646	lpxD	16	1.80594442	1	0.553726898
PA3649	PA3649	20	10.8356665	13	1.199741612
PA3675	PA3675	4	16.2534998	50	3.076260543
PA3738	xerD	9	9.02972209	8	0.885963036
PA3767	PA3767	6	1.80594442	9	4.98354208
PA3778	PA3778	6	1.80594442	7	3.876088284
PA3888	PA3888	6	5.41783325	19	3.506937019
PA3974	ladS	36	574.290325	842	1.466157383
PA4020	mpl	15	1.80594442	3	1.661180693
PA4045	PA4045	6	1.80594442	10	5.537268977
PA4110	ampC	21	37.9248328	125	3.295993439
PA4269	rpoC	49	1.80594442	8	4.429815182
PA4275	nusG	9	3.61188884	3	0.830590347
PA4277	tufB	23	1.80594442	6	3.322361386
PA4318	PA4318	7	10.8356665	69	6.367859324
PA4319	PA4319	13	21.671333	186	8.582766915
PA4320	PA4320	19	16.2534998	160	9.844033738
PA4321	PA4321	17	12.6416109	86	6.802930458
PA4322	PA4322	6	10.8356665	22	2.030331958
PA4323	PA4323	15	12.6416109	63	4.98354208
PA4351	PA4351	4	9.02972209	4	0.442981518
PA4413	ftsW	12	1.80594442	9	4.98354208
PA4417	murE	16	1.80594442	12	6.644722773
PA4422	PA4422	6	1.80594442	1	0.553726898
PA4423	PA4423	18	12.6416109	14	1.107453795
PA4424	PA4424	5	5.41783325	20	3.691512652
PA4428	sspA	12	7.22377767	26	3.599224835
PA4431	PA4431	8	0.1	3	30
PA4451	PA4451	2	0.1	1	10

PA4610	PA4610	1	5.41783325	5	0.922878163
PA4634	PA4634	8	3.61188884	17	4.706678631
PA4664	hemK	11	5.41783325	3	0.553726898
PA4671	PA4671	7	14.4475553	14	0.969022071
PA4726.1	PA4726.1	4	1.80594442	3	1.661180693
PA4729	panB	5	1.80594442	13	7.198449671
PA4793	PA4793	9	3.61188884	19	5.260405528
PA4795	PA4795	0	1.80594442	7	3.876088284
PA4853	fis	4	0.1	1	10
PA4890	desT	2	0.1	1	10
PA4932	rplI	4	1.80594442	7	3.876088284
PA4952	PA4952	5	1.80594442	3	1.661180693
PA4960	PA4960	11	3.61188884	11	3.045497938
PA5000	wapR	21	3.61188884	2	0.553726898
PA5005	PA5005	32	1.80594442	17	9.413357262
PA5016	aceF	7	5.41783325	7	1.292029428
PA5049	rpmE	7	18.0594442	18	0.996708416
PA5060	phaF	4	5.41783325	24	4.429815182
PA5113	PA5113	15	21.671333	62	2.860922305
PA5114	PA5114	37	61.4021102	320	5.211547273
PA5162	rmlD	11	1.80594442	6	3.322361386
PA5239	rho	10	5.41783325	20	3.691512652
PA5241	ppx	15	16.2534998	18	1.107453795
PA5259	hemD	13	3.61188884	5	1.384317244
PA5280	sss	8	3.61188884	4	1.107453795
PA5285	PA5285	1	1.80594442	5	2.768634489
PA5366	pstB	11	3.61188884	14	3.876088284
PA5405	PA5405	3	1.80594442	10	5.537268977
PA5409	PA5409	2	1.80594442	7	3.876088284

PA5555	atpG	15	0.1	2	20
--------	------	----	-----	---	----

<i>Genes with higher insertion frequency + B.t. WT</i>					
PA0285	PA0285	25	270.8916627	151	0.55741841
PA0427	oprM	21	0.1	3	30
PA0542	PA0542	0	14.44755534	4	0.276863449
PA0624	PA0624	4	25.28322185	8	0.31641537
PA0635	PA0635	4	16.25349976	4	0.246100843
PA0787	PA0787	5	21.67133301	6	0.276863449
PA0823	PA0823	0	1.805944418	1	0.553726898
PA0905	rsmA	4	30.7010551	10	0.325721705
PA1030.1	PA1030.1	2	0	0	N.D.
PA1082	flgG	6	83.07344322	21	0.252788366
PA1117	PA1117	1	0.1	1	10
PA1149	PA1149	3	7.223777672	5	0.692158622
PA1159	PA1159	3	0.1	4	40
PA1300	PA1300	2	21.67133301	7	0.323007357
PA1444	fliN	4	12.64161093	4	0.31641537
PA1612	PA1612	9	50.5664437	33	0.652606701
PA1635	kdpC	7	19.8653886	5	0.251694044
PA1644	PA1644	7	14.44755534	4	0.276863449
PA1692	PA1692	4	3.611888836	3	0.830590347
PA1718	pscE	0	16.25349976	4	0.246100843
PA1891	PA1891	4	14.44755534	3	0.207647587
PA2008	fahA	11	7.223777672	8	1.107453795
PA2066	PA2066	5	10.83566651	3	0.276863449
PA2145	PA2145	5	12.64161093	4	0.31641537
PA2161	PA2161	2	0.1	4	40
PA2198	PA2198	5	41.53672161	9	0.216675743

PA2312	PA2312	7	21.67133301	7	0.323007357
PA2315	PA2315	10	16.25349976	4	0.246100843
PA2334	PA2334	7	0.1	13	130
PA2351	PA2351	9	19.8653886	6	0.302032853
PA2469	PA2469	6	34.31294394	11	0.32057873
PA2492	mexT	8	2248.4008	677	0.301102899
PA2495	oprN	10	19.8653886	6	0.302032853
PA2497	PA2497	5	10.83566651	1	0.092287816
PA2614	lolA	5	1.805944418	1	0.553726898
PA2970	rpmF	5	3.611888836	9	2.49177104
PA3017	PA3017	3	12.64161093	3	0.237311528
PA3085	PA3085	2	10.83566651	2	0.184575633
PA3139.1	PA3139.1	3	0	0	N.D.
PA3181	PA3181	5	1.805944418	3	1.661180693
PA3194	edd	9	14.44755534	4	0.276863449
PA3411	PA3411	2	9.029722089	5	0.553726898
PA3448	PA3448	8	10.83566651	3	0.276863449
PA3480	PA3480	10	27.08916627	9	0.332236139
PA3520	PA3520	4	3.611888836	7	1.938044142
PA3808	PA3808	2	0.1	5	50
PA3813	iscU	3	5.417833254	2	0.369151265
PA3816	cysE	8	10.83566651	7	0.646014714
PA3833	PA3833	2	16.25349976	3	0.184575633
PA3844	PA3844	8	54.17833254	24	0.442981518
PA3937	PA3937	4	3.611888836	0	0
PA4033	PA4033	3	3.611888836	0	0
PA4092	hpaC	1	0	0	N.D.
PA4138	tyrS	10	28.89511069	14	0.484511036
PA4479	mreD	6	3.611888836	2	0.553726898

PA4482	gatC	2	0.1	1	10
PA4561	ribF	7	3.611888836	0	0
PA4637	PA4637	1	7.223777672	3	0.415295173
PA4663	moeB	9	0.1	1	10
PA4732	pgi	24	1.805944418	21	11.62826485
PA4822	PA4822	9	10.83566651	1	0.092287816
PA4856	retS	20	99.32694298	29	0.291965092
PA4916	PA4916	5	28.89511069	6	0.207647587
PA4918	PA4918	10	27.08916627	27	0.996708416
PA5062	PA5062	0	0	0	N.D.
PA5134	PA5134	11	27.08916627	5	0.184575633
PA5161	rmlB	19	0	0	N.D.
PA5183a	PA5183a	3	12.64161093	3	0.237311528
PA5203	gshA	25	2293.549411	700	0.305203802
PA5231	PA5231	27	12.64161093	3	0.237311528
PA5443	uvrD	22	14.44755534	4	0.276863449

1. Insertion counts are normalized by the total sequencing reads within each sample.
2. Genes with 3-fold more or greater difference in normalized insertion frequency in at least one of two replicate experiments and with at least 10 normalized insertions from one library in that experiment are included. Genes meeting these criteria in both replicates are highlighted in grey.
3. The gene was not detected in the wild-type sample.

Supplemental Table 2. Transposon sequencing-based analysis of *P. aeruginosa* fitness determinants during antagonism by *B. thai*.

		Normalized insertion counts			
Locus ID	Gene name	TA sites	+ <i>B.t.</i> WT	+ <i>B.t.</i> <i>tle3</i> ^{S264A}	Fold change (<i>tle3</i> ^{S264A} /WT)
<i>Genes with higher insertion frequency + B.t. tle3^{S264A}</i>					
PA0005	lptA	11	2	17.00958	8.504789999
PA0073	PA0073	4	0.1	34.01916	340.1916
PA0075	pppA	8	30	100.5111545	3.350371818
PA0079	PA0079	15	135	415.9615472	3.081196646
PA0171	PA0171	10	1	7.731627272	7.731627272
PA0180	cttP	5	3	52.5750654	17.5250218
PA0197	tonB2	2	5	24.74120727	4.948241454
PA0307	PA0307	7	65	231.9488182	3.568443356
PA0316	serA	13	21	85.04789999	4.0499
PA0402	pyrB	9	1	12.37060363	12.37060363
PA0407	gshB	10	7	26.28753272	3.755361818
PA0466	PA0466	1	0.1	27.83385818	278.3385818
PA0526	PA0526	1	38	160.8178473	4.232048612
PA0553	PA0553	2	0.1	12.37060363	123.7060363
PA0712	PA0712	4	7	24.74120727	3.534458181
PA0721	PA0721	4	0.1	12.37060363	123.7060363
PA0766	mucD	11	101	400.4982927	3.965329631
PA0909	PA0909	5	34	108.2427818	3.18361123
PA0928	gacS	18	3	9.277952726	3.092650909
PA0945	purM	13	32	123.7060363	3.865813636
PA0951a	PA0951a	1	6	57.21404181	9.535673635
PA0960	PA0960	0	10	34.01916	3.401916
PA0973	oprL	11	15	46.38976363	3.092650909

PA0974	PA0974	16	70	228.8561672	3.269373818
PA1013	purC	3	2	15.46325454	7.731627272
PA1034	PA1034	2	6	40.20446181	6.700743636
PA1101	fliF	16	421	1456.638578	3.459949116
PA1103	PA1103	2	0.1	35.56548545	355.6548545
PA1121	yfiR	7	21	83.50157454	3.976265454
PA1285	PA1285	6	12	43.29711272	3.608092727
PA1394	PA1394	0	11	37.1118109	3.373800991
PA1443	fliM	7	80	366.4791327	4.580989159
PA1547	PA1547	5	0.1	10.82427818	108.2427818
PA1548	PA1548	3	0.1	30.92650909	309.2650909
PA1549	PA1549	19	6	20.10223091	3.350371818
PA1550	PA1550	6	3	27.83385818	9.277952726
PA1554	ccoN1	25	211	638.6324127	3.026693899
PA1615	PA1615	5	11	35.56548545	3.23322595
PA1629	PA1629	5	21	80.40892363	3.828996363
PA1632	kdpF	3	2	10.82427818	5.41213909
PA1696	pscO	3	5	18.55590545	3.71118109
PA1715	pscB	2	2	6.185301817	3.092650909
PA1766	PA1766	13	8	54.1213909	6.765173863
PA1796.2	PA1796.2	2	0.1	13.91692909	139.1692909
PA1879	PA1879	2	2	10.82427818	5.41213909
PA2146	PA2146	1	0.1	24.74120727	247.4120727
PA2173	PA2173	0	0.1	34.01916	340.1916
PA2193	hcnA	2	1	12.37060363	12.37060363
PA2297	PA2297	3	17	58.76036727	3.456492192
PA2330	PA2330	3	2	21.64855636	10.82427818
PA2425	pvdG	13	8	24.74120727	3.092650909
PA2541	PA2541	5	9	46.38976363	5.154418181

PA2816	PA2816	1	31	114.4280836	3.691228504
PA2852	PA2852	9	6	20.10223091	3.350371818
PA2898	PA2898	1	4	17.00958	4.252395
PA2947	PA2947	2	18	69.58464545	3.865813636
PA2964	pabC	5	5	27.83385818	5.566771636
PA2992	PA2992	2	25	119.06706	4.762682399
PA3094.2	PA3094.2	3	2	12.37060363	6.185301817
PA3099	xcpV	1	8	29.38018363	3.672522954
PA3111	folC	15	5	20.10223091	4.020446181
PA3173	PA3173	11	11	44.84343818	4.076676198
PA3202	PA3202	3	10	34.01916	3.401916
PA3299	fadD1	19	22	98.96482908	4.498401322
PA3382	phnE	4	32	128.3450127	4.010781647
PA3509	PA3509	6	0.1	27.83385818	278.3385818
PA3574a	PA3574a	3	11	58.76036727	5.34185157
PA3738	xerD	9	9	34.01916	3.779906666
PA3815	iscR	7	13	51.02873999	3.925287692
PA4232	ssb	6	0.1	12.37060363	123.7060363
PA4275	nusG	9	8	61.85301817	7.731627272
PA4351	PA4351	4	9	41.75078727	4.638976363
PA4357	PA4357	1	21	80.40892363	3.828996363
PA4431	PA4431	8	2	17.00958	8.504789999
PA4451	PA4451	2	5	29.38018363	5.876036727
PA4726	cbrB	14	181	889.1371363	4.912359869
PA4726.1	PA4726.1	4	1	12.37060363	12.37060363
PA4752	ftsJ	9	9	32.47283454	3.608092727
PA4782	PA4782	2	39	119.06706	3.053001538
PA4853	fis	4	1	40.20446181	40.20446181
PA4890	desT	2	0.1	12.37060363	123.7060363

PA4894	PA4894	3	8	34.01916	4.252395
PA5000	wapR	21	6	24.74120727	4.123534545
PA5015	aceE	38	58	270.6069545	4.665637147
PA5016	aceF	7	3	18.55590545	6.185301817
PA5113	PA5113	15	198	632.4471108	3.194177327
PA5114	PA5114	37	218	3002.964032	13.77506437
PA5117	typA	13	13	66.49199454	5.114768811
PA5148	PA5148	5	33	149.9935691	4.545259669
PA5162	rmlD	11	6	40.20446181	6.700743636
PA5198	PA5198	9	4	12.37060363	3.092650909
PA5260	hemC	8	0.1	12.37060363	123.7060363
PA5285	PA5285	1	8	57.21404181	7.151755226
PA5366	pstB	11	1	6.185301817	6.185301817

<i>Genes with higher insertion frequency + B.t. WT</i>					
PA0006	PA0006	13	156	34.01916	0.218071538
PA0125	PA0125	2	40	12.37060363	0.309265091
PA0871	phhB	4	225	41.75078727	0.185559055
PA1045	PA1045	17	6	1.546325454	0.257720909
PA1112a	PA1112a	1	55	12.37060363	0.224920066
PA1117	PA1117	1	47	12.37060363	0.263204333
PA1149	PA1149	3	86	20.10223091	0.233746871
PA1446	fliP	3	161	46.38976363	0.288135178
PA1503	PA1503	4	78	23.19488182	0.29737028
PA1571	PA1571	2	48	7.731627272	0.161075568
PA1664	PA1664	2	17	0.1	0.005882353
PA1685	masA	10	30	9.277952726	0.309265091
PA1742	PA1742	12	129	32.47283454	0.2517274
PA1743	PA1743	3	42	6.185301817	0.147269091

PA1802	clpX	20	19	6.185301817	0.325542201
PA1842	PA1842	2	72	23.19488182	0.322151136
PA1995	PA1995	3	33	10.82427818	0.32800843
PA2003	bdhA	3	112	35.56548545	0.317548977
PA2007	maiA	8	455	106.6964564	0.234497706
PA2008	fahA	11	174	18.55590545	0.106643135
PA2143	PA2143	2	88	10.82427818	0.123003161
PA2183	PA2183	3	58	18.55590545	0.319929404
PA2187	PA2187	6	116	24.74120727	0.21328627
PA2357	msuE	7	112	37.1118109	0.331355455
PA2492	mexT	8	17782	4741.033843	0.266619831
PA2614	lolA	5	63	20.10223091	0.31908303
PA2967	fabG	8	11	1.546325454	0.140575041
PA3139.1	PA3139.1	3	17	0.1	0.005882353
PA3165	hisC2	15	32	0.1	0.003125
PA3368.1	PA3368.1	3	35	6.185301817	0.176722909
PA3520	PA3520	4	56	13.91692909	0.248516591
PA3557	arnE	1	18	3.092650909	0.171813939
PA3721	nalC	8	6	1.546325454	0.257720909
PA3808	PA3808	2	46	12.37060363	0.268926166
PA3813	iscU	3	39	1.546325454	0.039649371
PA3821	secD	16	10	0.1	0.01
PA3822	PA3822	3	12	0.1	0.008333333
PA4092	hpaC	1	38	6.185301817	0.1627711
PA4236	katA	23	2815	896.8687635	0.318603468
PA4561	ribF	7	27	4.638976363	0.171813939
PA4662	murI	15	30	3.092650909	0.103088364
PA4758	carA	17	5	1.546325454	0.309265091
PA5062	PA5062	0	21	3.092650909	0.147269091

PA5134	PA5134	11	319	94.32585272	0.295692328
--------	--------	----	-----	-------------	-------------

Supplemental Table 3. Transposon sequencing-based analysis of *P. aeruginosa* fitness determinants during antagonism by *B. thai*.

		Normalized insertion counts			
Locus ID	Gene name	TA sites	+ <i>B.t.</i> WT	+ <i>B.t.</i> $\Delta colA$	Fold change ($\Delta colA$ /WT)
<i>Genes with higher insertion frequency + B.t. $\Delta colA$</i>					
PA0005	lptA	11	2	7.928575216	3.964287608
PA0037	trpI	8	237	767.4860809	3.238337894
PA0180	cttP	5	3	17.44286548	5.814288492
PA0197	tonB2	2	5	25.37144069	5.074288138
PA0407	gshB	10	7	25.37144069	3.624491527
PA0466	PA0466	1	0	11.1000053	N.D.
PA0526	PA0526	1	38	185.5286601	4.88233316
PA0712	PA0712	4	7	33.30001591	4.75714513
PA0753	PA0753	5	15	63.42860173	4.228573449
PA0928	gacS	18	3	9.51429026	3.171430087
PA0947	PA0947	7	7	22.20001061	3.171430087
PA0960	PA0960	0	10	44.40002121	4.440002121
PA0973	oprL	11	15	57.08574156	3.805716104
PA1034	PA1034	2	6	49.15716634	8.192861057
PA1045	PA1045	17	6	30.12858582	5.02143097
PA1121	yfiR	7	21	77.70003712	3.700001768
PA1233	PA1233	5	16	49.15716634	3.072322896
PA1394	PA1394	0	11	33.30001591	3.027274174
PA1548	PA1548	3	0	14.27143539	N.D.
PA1550	PA1550	6	3	9.51429026	3.171430087
PA1552.1	ccQ1	2	0	26.95715574	N.D.
PA1564	PA1564	2	0	12.68572035	N.D.
PA1645	PA1645	5	9	36.471446	4.052382888

PA1696	pscO	3	5	42.81430617	8.562861234
PA1747	PA1747	1	0	15.85715043	N.D.
PA1796.2	PA1796.2	2	0	12.68572035	N.D.
PA1816	dnaQ	8	0	15.85715043	N.D.
PA1879	PA1879	2	2	19.02858052	9.51429026
PA2176	PA2176	4	17	52.32859643	3.078152731
PA2193	hcnA	2	1	20.61429556	20.61429556
PA2321	PA2321	3	1	26.95715574	26.95715574
PA2330	PA2330	3	2	11.1000053	5.550002651
PA2425	pvdG	13	8	39.64287608	4.95535951
PA2541	PA2541	5	9	30.12858582	3.347620647
PA2554	PA2554	3	11	47.5714513	4.324677391
PA2724	PA2724	4	41	161.7429344	3.94494962
PA2738	himA	3	4	12.68572035	3.171430087
PA2743	infC	12	2	6.342860173	3.171430087
PA2805	PA2805	0	6	20.61429556	3.435715927
PA2855	PA2855	3	15	45.98573625	3.06571575
PA2895	PA2895	1	9	28.54287078	3.171430087
PA2898	PA2898	1	4	15.85715043	3.964287608
PA2914	PA2914	5	33	115.7571982	3.507793884
PA2947	PA2947	2	18	63.42860173	3.523811207
PA2964	pabC	5	5	19.02858052	3.805716104
PA2991	sth	18	0	14.27143539	N.D.
PA2992	PA2992	2	25	98.31433268	3.932573307
PA3051	PA3051	2	5	17.44286548	3.488573095
PA3067	PA3067	1	0	25.37144069	N.D.
PA3094.2	PA3094.2	3	2	23.78572565	11.89286282
PA3099	xcpV	1	8	34.88573095	4.360716369
PA3111	folC	15	5	42.81430617	8.562861234

PA3133.4	PA3133.4	3	0	14.27143539	N.D.
PA3145	wbpL	34	1	9.51429026	9.51429026
PA3205	PA3205	1	5	20.61429556	4.122859113
PA3382	phnE	4	32	115.7571982	3.617412442
PA3385	amrZ	3	20	61.84288669	3.092144334
PA3574a	PA3574a	3	11	53.91431147	4.901301043
PA3634	PA3634	2	4	14.27143539	3.567858847
PA3640	dnaE	46	2	15.85715043	7.928575216
PA3649	PA3649	20	22	74.52860703	3.387663956
PA3815	iscR	7	13	49.15716634	3.781320488
PA3879	narL	2	31	123.6857734	3.989863657
PA4020	mpl	15	1	3.171430087	3.171430087
PA4275	nusG	9	8	71.35717695	8.919647118
PA4277	tufB	23	2	6.342860173	3.171430087
PA4319	PA4319	13	95	307.6287184	3.238197036
PA4320	PA4320	19	70	274.3287025	3.918981464
PA4322	PA4322	6	22	115.7571982	5.261690825
PA4323	PA4323	15	27	107.8286229	3.993652702
PA4351	PA4351	4	9	47.5714513	5.285716811
PA4413	ftsW	12	9	50.74288138	5.638097932
PA4422	PA4422	6	0	14.27143539	N.D.
PA4431	PA4431	8	2	6.342860173	3.171430087
PA4452	PA4452	2	11	49.15716634	4.468833304
PA4459	PA4459	13	9	31.71430087	3.523811207
PA4610	PA4610	1	17	53.91431147	3.171430087
PA4671	PA4671	7	2	11.1000053	5.550002651
PA4672	PA4672	5	3	12.68572035	4.228573449
PA4726.1	PA4726.1	4	1	17.44286548	17.44286548
PA4820	PA4820	5	9	26.95715574	2.995239526

PA4853	fis	4	1	19.02858052	19.02858052
PA4890	desT	2	0	20.61429556	N.D.
PA4894	PA4894	3	8	52.32859643	6.541074553
PA4933	PA4933	10	7	22.20001061	3.171430087
PA4952	PA4952	5	4	26.95715574	6.739288934
PA5000	wapR	21	6	25.37144069	4.228573449
PA5016	aceF	7	3	22.20001061	7.400003535
PA5049	rpmE	7	4	22.20001061	5.550002651
PA5148	PA5148	5	33	111.000053	3.363637971
PA5162	rmlD	11	6	45.98573625	7.664289376
PA5198	PA5198	9	4	17.44286548	4.360716369
PA5199	amgS	9	3	23.78572565	7.928575216
PA5285	PA5285	1	8	34.88573095	4.360716369

<i>Genes with higher insertion frequency + B.t. WT</i>					
PA0006	PA0006	13	156	41.22859113	0.264285841
PA0125	PA0125	2	40	7.928575216	0.19821438
PA0420	bioA	19	45	12.68572035	0.281904897
PA0666	PA0666	10	127	36.471446	0.28717674
PA0715	PA0715	61	14	3.171430087	0.22653072
PA0763	mucA	9	52	15.85715043	0.304945201
PA0905.3	PA0905.3	4	10	1.585715043	0.158571504
PA0913	mgtE	10	96	23.78572565	0.247767976
PA1030.1	PA1030.1	2	55	15.85715043	0.288311826
PA1117	PA1117	1	47	1.585715043	0.033738618
PA1149	PA1149	3	86	12.68572035	0.147508376
PA1159	PA1159	3	32	9.51429026	0.297321571
PA1801	clpP	12	22	6.342860173	0.288311826
PA1845	PA1845	4	184	58.6714566	0.318866612
PA1985	pqqA	1	12	0.1	0.008333333

PA2142a	PA2142a	2	50	9.51429026	0.190285805
PA2187	PA2187	6	116	36.471446	0.314409017
PA2375	PA2375	1	32	9.51429026	0.297321571
PA2421	PA2421	16	302	99.90004773	0.33079486
PA2645	nuoJ	8	145	45.98573625	0.317143009
PA2778	PA2778	7	325	104.6571929	0.322022132
PA2967	fabG	8	11	0.1	0.009090909
PA2970	rpmF	5	30	7.928575216	0.264285841
PA3014	faoA	19	17	0.1	0.005882353
PA3139.1	PA3139.1	3	17	4.75714513	0.279832066
PA3151	hisF2	27	19	3.171430087	0.166917373
PA3165	hisC2	15	32	9.51429026	0.297321571
PA3482	metG	25	71	20.61429556	0.290342191
PA3496	PA3496	1	71	12.68572035	0.178672118
PA3808	PA3808	2	46	6.342860173	0.137888265
PA3821	secD	16	10	3.171430087	0.317143009
PA3844	PA3844	8	898	247.3715468	0.275469428
PA4092	hpaC	1	38	0	0
PA4236	katA	23	2815	829.3289676	0.294610646
PA4479	mreD	6	56	17.44286548	0.311479741
PA4581.1	PA4581.1	2	21	6.342860173	0.302040961
PA4663	moeB	9	28	3.171430087	0.11326536
PA5114	PA5114	37	218	55.50002651	0.254587278
PA5134	PA5134	11	319	71.35717695	0.22369021
PA5223	ubiH	14	36	7.928575216	0.2202382
PA5241	ppx	15	10	3.171430087	0.317143009

Supplemental Table 4. Mass spectrometric analysis of *P. aeruginosa* Arc3A and Arc3B immunoprecipitation samples.

Locus ID ¹	Peptide counts of sample (%) ²	Fold change (VSV-G/Ctrl ³)
Arc3A-VSV-G sample		
PA5113 (Arc3A)	5.86	>200
PA4385	1.62	2.29
PA5016	1.45	0.82
PA0090	1.17	0.72
PA3729	1.12	1.30
PA4761	1.12	0.71
PA5114 (Arc3B)	1.12	N.D. ⁴
PA5239	1.06	1.10
PA3861	1.00	1.10
PA4269	1.00	1.10
PA1092	0.95	0.78
PA0141	0.89	0.71
PA0963	0.84	1.27
PA2976	0.84	0.83
PA4260	0.84	0.69
PA4265	0.84	0.61
PA4270	0.84	1.04
PA1803	0.78	0.74
PA2151	0.78	0.77
PA3950	0.78	1.19
PA3001	0.73	1.10
PA3656	0.73	0.80
PA5173	0.73	0.76
PA5554	0.73	1.20
PA5556	0.73	2.05

Arc3B-VSV-G sample		
PA5554	2.92	4.81
PA5113 (Arc3A)	2.22	>200
PA5114 (Arc3B)	1.44	N.D.
PA4751	1.30	12.87
PA5556	1.26	3.55
PA3729	1.10	1.28
PA5016	1.10	0.62
PA4429	0.99	N.D.
PA4942	0.96	6.36
PA2493	0.92	2.60
PA3160	0.90	N.D.
PA4246	0.87	0.79
PA0090	0.85	0.53
PA1552	0.83	N.D.
PA0077	0.81	5.33
PA2494	0.81	ND
PA2976	0.72	0.71
PA0659	0.70	N.D.
PA4761	0.70	0.44
PA4941	0.65	2.57
PA4265	0.63	0.46
PA3656	0.61	0.67
PA3794	0.61	N.D.
PA2151	0.56	0.55
PA3821	0.56	N.D.

1. Proteins containing at least two peptides identified in a given immunoprecipitation sample are included. Arc3A and Arc3B are highlighted in grey.

2. Value corresponds to the abundance (peptide counts) of the protein within the total immunoprecipitation sample. Only the 25 most abundant proteins in each sample are shown.
3. Immunoprecipitation from a *P. aeruginosa* strain lacking a VSV-G-tagged protein served as the control sample (Ctrl).
4. The protein was not detected in the control sample.

Supplemental Table 5. Bacterial strains, Oligonucleotides, Plasmids used in the study.

Bacterial strains	Reference
<i>Pseudomonas aeruginosa</i> PAO1	36
<i>Pseudomonas aeruginosa</i> PAO1 Δ pa2541	This study
<i>Pseudomonas aeruginosa</i> PAO1 Δ pa2541 Δ pa2536	This study
<i>Pseudomonas aeruginosa</i> PAO1 Δ pa4323	This study
<i>Pseudomonas aeruginosa</i> PAO1 Δ pa4323 Δ pa4320	This study
<i>Pseudomonas aeruginosa</i> PAO1 Δ pa5114	This study
<i>Pseudomonas aeruginosa</i> PAO1 Δ pa5114 Δ pa5113	This study
<i>Pseudomonas aeruginosa</i> PAO1 Δ pa2541, <i>Tn7::AraE::pa2541</i>	This study
<i>Pseudomonas aeruginosa</i> PAO1 Δ pa4323, <i>Tn7::AraE::pa4323</i>	This study
<i>Pseudomonas aeruginosa</i> PAO1 Δ pa5114, <i>Tn7::AraE::pa5114</i>	This study
<i>Pseudomonas aeruginosa</i> PAO1 Δ pa2541 Δ pa4323 Δ pa5114	This study
<i>Pseudomonas aeruginosa</i> PAO1 Δ gacS (Δ pa0928)	5
<i>Pseudomonas aeruginosa</i> PAO1 Δ icmF1 (Δ pa0077)	55
<i>Pseudomonas aeruginosa</i> PAO1 Δ pa5112	This study
<i>Pseudomonas aeruginosa</i> PAO1 Δ pa5114, <i>Tn7::AraE::empty</i>	This study
<i>Pseudomonas aeruginosa</i> PAO1 Δ pa5114, <i>Tn7::AraE::pfl_rs01995</i>	This study
<i>Pseudomonas aeruginosa</i> PAO1 Δ pa5114, <i>Tn7::AraE::i35_rs27920</i>	This study
<i>Pseudomonas aeruginosa</i> PAO1 Δ pa5114, <i>Tn7::AraE::pspto_rs26695</i>	This study
<i>Pseudomonas aeruginosa</i> PAO1 Δ pa5114, <i>Tn7::AraE::ta05_rs00690</i>	This study
<i>Pseudomonas aeruginosa</i> PAO1 Δ pa3267	This study
<i>Pseudomonas aeruginosa</i> PAO1 Δ pa5114 Δ pa3267	This study
<i>Pseudomonas aeruginosa</i> PAO1 Δ retS (Δ pa4856)	56
<i>Pseudomonas aeruginosa</i> PAO1 Δ retS Δ pa3267	This study
<i>Pseudomonas aeruginosa</i> PAO1 Δ retS Δ pa5114	This study
<i>Pseudomonas aeruginosa</i> PAO1 Δ rpoS (Δ pa3622)	22
<i>Pseudomonas aeruginosa</i> PAO1 Δ vacJ (Δ pa2800)	23
<i>Pseudomonas aeruginosa</i> PAO1 Δ pa2541_vsv-g	This study
<i>Pseudomonas aeruginosa</i> PAO1 Δ retS, Δ pa2541_vsv-g	This study
<i>Pseudomonas aeruginosa</i> PAO1 Δ gacS, Δ pa2541_vsv-g	This study
<i>Pseudomonas aeruginosa</i> PAO1 Δ pa4323_vsv-g	This study
<i>Pseudomonas aeruginosa</i> PAO1 Δ retS, Δ pa4323_vsv-g	This study
<i>Pseudomonas aeruginosa</i> PAO1 Δ gacS, Δ pa4323_vsv-g	This study
<i>Pseudomonas aeruginosa</i> PAO1 Δ pa5114_vsv-g	This study
<i>Pseudomonas aeruginosa</i> PAO1 Δ retS, Δ pa5114_vsv-g	This study

<i>Pseudomonas aeruginosa</i> PAO1 $\Delta gacS, pa5114$ vsv-g	This study
<i>Pseudomonas aeruginosa</i> PAO1 $\Delta retS, pa5113$ vsv-g	This study
<i>Burkholderia thailandensis</i> E264 (ATCC 700388)	37
<i>Burkholderia thailandensis</i> E264 $\Delta icmF1$ (ΔBTH I2954)	5
<i>Burkholderia thailandensis</i> E264 $tle3^{S264A}$ (BTH II0090 S264A + BTH I3226 S264A)	This study
<i>Burkholderia thailandensis</i> E264 $tle1^{S267A}$ (BTH I2698 S267A + BTH I2701 S267A)	This study
<i>Burkholderia thailandensis</i> E264 $\Delta colA$ (ΔBTH I2691)	This study
<i>Burkholderia thailandensis</i> E264 $\Delta tae2$ (ΔBTH I0068)	26
<i>Burkholderia thailandensis</i> E264 $Tn7::Tp-PS12-mCherry$	43
<i>Burkholderia thailandensis</i> E264 $tle3$ sensitized strain (ΔBTH I3225-8, ΔBTH II0089-94)	This study
<i>Burkholderia thailandensis</i> E264 $Tn7::Tp-PS12-mCherry$ $tle3$ sensitized strain (ΔBTH I3225-8, ΔBTH II0089-94)	This study
<i>Pseudomonas protegens</i> pf-5 (ATCC BAA-477)	38
<i>Pseudomonas protegens</i> pf-5 Δpfl rs01995	This study
<i>Escherichia coli</i> DH5 α	Thermo Fisher Scientific Cat# 18258012
<i>Escherichia coli</i> SM10	Biomedal Lifescience Cat# BS-3303
<i>Escherichia coli</i> UE54	53
MG1655 $lpp-2\Delta ara714$ $rcsF::mini-Tn10$ cam $pgsA::FRT$ - $kan-FRT$	

Oligonucleotides 5'-3'	Source
pEXG2_ΔPA2541_F1 CAAGCTTCTGCAGGTCGACTCTAGAAGGTGGAACCG GACCTGAAG	Integrated DNA Technology
pEXG2_ΔPA2541_R1 CTCAGGCCTGGAAATCATGTCAGCCAGTCC	Integrated DNA Technology
pEXG2_ΔPA2541_F2 CATGATTCCCAGGCCTGAGAGAGGAACG	Integrated DNA Technology
pEXG2_ΔPA2541_R2 TAAGGTACCGAATTGAGCTCGTATGACCCAGGC TCG	Integrated DNA Technology
pEXG2_ΔPA4323_F1 AGCTCGAGCCGGGATCCTCTAGAGACGCAGAAC CGATCGAG	Integrated DNA Technology
pEXG2_ΔPA4323_R1 AAAGCACGCCGATGGCTTCATACGCCGG	Integrated DNA Technology
pEXG2_ΔPA4323_F2 GAAGCCATCGGGCGTGCTTGACGGATC	Integrated DNA Technology
pEXG2_ΔPA4323_R2 GGAAGCATAAATGTAAAGCAAGCTTGAGCGATGCC GAGCTGGA	Integrated DNA Technology

pEXG2_ΔPA5114_F1 CAAGCTTCTGCAGGTCGACTCTAGAGCCGCATGCCCTTGACCT	Integrated DNA Technology
pEXG2_ΔPA5114_R1 CGACCTCGGCAATCCATTGCATGCGTCGAATC	Integrated DNA Technology
pEXG2_ΔPA5114_F2 GCAATGGATTGCCGAGGGTCGCATCGGAG	Integrated DNA Technology
pEXG2_ΔPA5114_R2 AATTGAGCTCACCAAGATCATCGGCGCCG	Integrated DNA Technology
pEXG2_ΔPA2536_F1 CAAGCTTCTGCAGGTCGACTCTAGACTCGGCCTGGCCCGAGC	Integrated DNA Technology
pEXG2_ΔPA2536_R1 CAGGCGAACCTCAGGGCGTTCGTTCATCTCAGGCCCT	Integrated DNA Technology
pEXG2_ΔPA2536_F2 GGAGGCCTGAGATGAACGAAACGCCCTGAGGTTCGCCTG	Integrated DNA Technology
pEXG2_ΔPA2536_R2 TAAGGTACCGAATTGAGCTCCACATCGGTCTCAGCGAAC	Integrated DNA Technology
pEXG2_ΔPA4320_F1 AGCTCGAGCCGGGATCCTCTAGATGTTGGCTTCATCATGAAC	Integrated DNA Technology
pEXG2_ΔPA4320_R1 TGCAGCCCACGCTGGCGTCAGTCAG	Integrated DNA Technology
pEXG2_ΔPA4320_F2 CGCCAGCGTGGCTGGCGCAGCCTTTC	Integrated DNA Technology
pEXG2_ΔPA4320_R2 GGAAGCATAAAATGTAAAGCAAGCTTGTGGCGGTTTCTCGCT	Integrated DNA Technology
pEXG2_ΔPA5114/PA5113_F1 CAAGCTTCTGCAGGTCGACTCTAGAGCCGCATGCCCTTGACCT	Integrated DNA Technology
pEXG2_ΔPA5114/PA5113_R1 TGTTCGCGAAATCCAATTGCATGCGTCGAATC	Integrated DNA Technology
pEXG2_ΔPA5114/PA5113_F2 GCAATGGATTTCGCCAACAGCCATGAG	Integrated DNA Technology
pEXG2_ΔPA5114/PA5113_R2 TAAGGTACCGAATTGAGCTAACAGCCAGACCACGATGTAGC	Integrated DNA Technology
pEXG2_ΔPA5113_F1 CAAGCTTCTGCAGGTCGACTCTAGATTGCTAGGGGTGCTGGCG	Integrated DNA Technology
pEXG2_ΔPA5113_R1 ATGGCTTGTGGAGCGCGTCATGGCTGC	Integrated DNA Technology

pEXG2_ΔPA5113_F2 GACGCGCTCCAACAAGCCATGAGGCCGGTTC	Integrated DNA Technology
pEXG2_ΔPA5113_R2 TAAGGTACCGAATTGAGCTAACAGCCAGACCACG ATGTAG	Integrated DNA Technology
pEXG2_ΔPA5112_F1 CAAGCTTCTGCAGGTGACTCTAGATACCGCTGGCA GTTGCCG	Integrated DNA Technology
pEXG2_ΔPA5112_R1 AGAAGTCCAGCGCCATTCTGATCATTCTCTTACTC	Integrated DNA Technology
pEXG2_ΔPA5112_F2 CAGAATGGCGCTGGACTTCTGAAACGGCGGC	Integrated DNA Technology
pEXG2_ΔPA5112_R2 TAAGGTACCGAATTGAGCTCCCGCAACCGCCGGT TGG	Integrated DNA Technology
pEXG2_ΔPA3267_F1 CAAGCTTCTGCAGGTGACTCTAGATCTACATCGAC TTCGACG	Integrated DNA Technology
pEXG2_ΔPA3267_R1 ATCAGCGAGCTGGTCATCGCCTTGTAC	Integrated DNA Technology
pEXG2_ΔPA3267_F2 GATGACCCAAGCTGCTGATCGATCCGC	Integrated DNA Technology
pEXG2_ΔPA3267_R2 TAAGGTACCGAATTGAGCTTCGCCGGCCTGTC GAAG	Integrated DNA Technology
pEXG2_APFL_RS01995_F1 CAAGCTTCTGCAGGTGACTCTAGAAACTACAACGT CAGCCTG	Integrated DNA Technology
pEXG2_APFL_RS01995_R1 TTCATTCAACGGTTGCCTATCCATTGCATGTGTCG	Integrated DNA Technology
pEXG2_APFL_RS01995_F2 CGACACATGCAATGGATAGGCAAACCGTTGAATGAA	Integrated DNA Technology
pEXG2_APFL_RS01995_R2 TAAGGTACCGAATTGAGCTCCCTGCGACCACACCAG CG	Integrated DNA Technology
pEXG2_PA2541_VSVG_F1 CAAGCTTCTGCAGGTGACTCTAGAGCGCTGATACG GACCATGC	Integrated DNA Technology
pEXG2_PA2541_VSVG_R1 TTTCCTTAATCTATTCAATATCTGTATAGGCC TGGCCGTCGCTGCCCG	Integrated DNA Technology
pEXG2_PA2541_VSVG_F2 TATACAGATATTGAAATGAATAGATTAGGAAAATGA GAGGGAACGGCGAAC	Integrated DNA Technology

pEXG2_PA2541_VSVG_R2 TAAGGTACCGAATTGAGCTCCTGCAGCGCACG ATG	Integrated DNA Technology
pEXG2_PA4323_VSVG_F1 CAAGCTTCTGCAGGTCGACTCTAGATGGAGTTCCAC CAGTTGCGCG	Integrated DNA Technology
pEXG2_PA4323_VSVG_R1 TGATCCGTCATTTCCTAATCTATTCAATATCT GTATAAAGCACGCCGGCGCGCT	Integrated DNA Technology
pEXG2_PA4323_VSVG_F2 TATACAGATATTGAAATGAATAGATTAGGAAAATGA CGGATCAGACCGACTG	Integrated DNA Technology
pEXG2_PA4323_VSVG_R2 TAAGGTACCGAATTGAGCTCAAGGTACACTTCTCC GCC	Integrated DNA Technology
pEXG2_PA5114_VSVG_F1 CAAGCTTCTGCAGGTCGACTCTAGACTGGAGCTGCG CTACCTGTCG	Integrated DNA Technology
pEXG2_PA5114_VSVG_R1 TAATCTATTCAATTCAATATCTGTATATGGCTGCTCG GCCTCCGA	Integrated DNA Technology
pEXG2_PA5114_VSVG_F2 GATATTGAAATGAATAGATTAGGAAAATCGGAGGCC GAGCAGCCA	Integrated DNA Technology
pEXG2_PA5114_VSVG_R2 TAAGGTACCGAATTGAGCTCGCTCGGACCAAGATCA TCGGC	Integrated DNA Technology
pEXG2_PA5113_VSVG_F1 CAAGCTTCTGCAGGTCGACTCTAGACTGCGTCTGGC CTGGCCG	Integrated DNA Technology
pEXG2_PA5113_VSVG_R1 TTTCCTAATCTATTCAATTATCTGTATATGGCT TGTCGGCGAGGAAC	Integrated DNA Technology
pEXG2_PA5113_VSVG_F2 TATACAGATATTGAAATGAATAGATTAGGAAAATGA GCCGGTCCGCGCTATG	Integrated DNA Technology
pEXG2_PA5113_VSVG_R1 TAAGGTACCGAATTGAGCTCGTCGGCAACAGCCA GAC	Integrated DNA Technology
pUC18_PA2541_F AGC GAATTCGAGCTCGGTACCAACGGGAGGAAAG ATGATTCCGTCTATCAACTC	Integrated DNA Technology
pUC18_PA2541_R CTCATCCGCCAAACAGCCAAGCTTCAGGCCTGGC CGTCGC	Integrated DNA Technology

pUC18_PA4323_F AGCGAATCGAGCTCGGTACCACGGGAGGAAAGAT GAAGCCATCGCGGCCCTGCTGG	Integrated DNA Technology
pUC18_PA4323_R CTCATCCGCCAAAACAGCCAAGCTTCAAAGCACGC CGGCGCGCTTCCAG	Integrated DNA Technology
pUC18_PA5114_F AGCGAATCGAGCTCGGTACCACGGGAGGAAAGAT GCAATGGATTTCATGCTGG	Integrated DNA Technology
pUC18_PA5114_R CTCATCCGCCAAAACAGCCAAGCTTCATGGCTGCT CGGCCTC	Integrated DNA Technology
pUC18_pfl_rs01995_F AGCGAATCGAGCTCGGTACCACGGGAGGAAAGAT GCAATGGATATTGATGCTGC	Integrated DNA Technology
pUC18_pfl_rs01995_R CTCATCCGCCAAAACAGCCAAGCTTCACGATGACA CTCCTTCATTC	Integrated DNA Technology
pUC18_i35_rs27920_F AGCGAATCGAGCTCGGTACCACGGGAGGAAAGAT GAACTGGGCATTCGCCG	Integrated DNA Technology
pUC18_i35_rs27920_R CTCATCCGCCAAAACAGCCAAGCTTCATGGCTGGC CGTCCTG	Integrated DNA Technology
pUC18_pspto_rs26695_F AGCGAATCGAGCTCGGTACCACGGGAGGAAAGAT GCTTTGGATTGTCTGGTAG	Integrated DNA Technology
pUC18_pspto_rs26695_R CTCATCCGCCAAAACAGCCAAGCTTCATGGCGTT CAGGCGCTG	Integrated DNA Technology
pUC18_ta05_rs00690_F AGCGAATCGAGCTCGGTACCACGGGAGGAAAGAT GGACGACCTTTAACCTG	Integrated DNA Technology
pUC18_ta05_rs00690_R CTCATCCGCCAAAACAGCCAAGCTTCATTGTTTC TCCAGCTTG	Integrated DNA Technology
pJRC115_BTH_II0090 ^{S264A} _F1 TAAAACGACGCCAGTGCAAGCTCGACGGATCAG CGTTCAAGCTGC	Integrated DNA Technology
pJRC115_BTH_II0090 ^{S264A} _R1 ACCTTGGGCATGACCCATCACCGTGATCGTTCGTG	Integrated DNA Technology
pJRC115_BTH_II0090 ^{S264A} _F2 GGTCATGCCAAGGTACGATCATCACGCTGCTCG	Integrated DNA Technology
pJRC115_BTH_II0090 ^{S264A} _R2 GCTCGGTACCCGGGGATCCTCTAGACGGCTCGGCAC GATGCGC	Integrated DNA Technology

pJRC115_BTH_I3226 ^{S264A} _F1 TAAAAACGACGCCAGTGCCAAGCTCGACGGATCAG CGTTCAAGCTGC	Integrated DNA Technology
pJRC115_BTH_I3226 ^{S264A} _R1 ACCTTGGCATGACCATCACCGTATCGTTCTG	Integrated DNA Technology
pJRC115_BTH_I3226 ^{S264A} _F2 GGTCATGCCAAGGTACGATCATCACGCTGCTCG	Integrated DNA Technology
pJRC115_BTH_I3226 ^{S264A} _R2 GCTCGGTACCCGGGGATCCTCTAGACGGCTCGCAC GATGCGC	Integrated DNA Technology
pJRC115_BTH_I2698 ^{S267A} _F1 TCAATCAGTATCTAGAGGGACACCTTCTCAAGCGA AATC	Integrated DNA Technology
pJRC115_BTH_I2698 ^{S267A} _R1 GCCGCGCGCAAACCAACACATAAAGGCGAATGC G	Integrated DNA Technology
pJRC115_BTH_I2698 ^{S267A} _F2 GGTTTCGCGCGCGCGCAGCGGAAGCTCGCACGTT TC	Integrated DNA Technology
pJRC115_BTH_I2698 ^{S267A} _R2 TGTAAAGCTAGAATTCCATCAAACCCGCTGTCCCAT GCTC	Integrated DNA Technology
pJRC115_BTH_I2701 ^{S267A} _F1 TAAAAACGACGCCAGTGCCAAGCTTGAAAGACGAG CAGGACGCG	Integrated DNA Technology
pJRC115_BTH_I2701 ^{S267A} _R1 ACCCCGCGCAAACCGAATACGTATAGCCGAATGCG	Integrated DNA Technology
pJRC115_BTH_I2701 ^{S267A} _F2 GGTTTCGCGCGGGGTGCAGCGGAGGCTCGCAC	Integrated DNA Technology
pJRC115_BTH_I2701 ^{S267A} _R2 GCTCGGTACCCGGGGATCCTCTAGACTCGACCTCCA GCAGATCG	Integrated DNA Technology
pJRC115_ABTH_I2691_F1 TAAAAACGACGCCAGTGCCAAGCTTATTCAAGCGC GGCCAGTC	Integrated DNA Technology
pJRC115_ABTH_I2691_R1 ATCTATGCGAGCTTCCGCCATTAAATTCC	Integrated DNA Technology
pJRC115_ABTH_I2691_F2 GGCGGGAAGCTCGCATAGATGAGTGATG	Integrated DNA Technology
pJRC115_ABTH_I2691_R2 GCTCGGTACCCGGGGATCCTCTAGATTCTGTCAATA CTTAAATACAATTTC	Integrated DNA Technology
pJRC115_ABTH_II0089-94_F1 TAAAAACGACGCCAGTGCCAAGCTGAATCAGTGCA TCGCTGTAC	Integrated DNA Technology

pJRC115_ΔBTH_II0089-94_R1 ATGTTTGCTTAGCGTATCGTCAAATTGG	Integrated DNA Technology
pJRC115_ΔBTH_II0089-94_F2 CGATACGCTAACGAAAACATGAGATTATTGAAGAG	Integrated DNA Technology
pJRC115_ΔBTH_II0089-94_R2 GCTCGGTACCCGGGGATCCTCTAGATATGCAACGCA TTGCCGAAAC	Integrated DNA Technology
pJRC115_ΔBTH_I3225-8_F1 TAAAACGACGGCCAGTGCCAAGCTTCCGGTCAATAT ACCACCATC	Integrated DNA Technology
pJRC115_ΔBTH_I3225-8_R1 ATGTGCGCCCCGTATCGTCAAATTGGTCAC	Integrated DNA Technology
pJRC115_ΔBTH_I3225-8_F2 GAACGATAACGGGGCGCACATAATAAGACTTG	Integrated DNA Technology
pJRC115_ΔBTH_I3225-8_R2 GCTCGGTACCCGGGGATCCTCTAGAATTGCTGTTTC TGCTGATG	Integrated DNA Technology
PCR_1A GTCTCGTGGCTCGGAGATGTGTATAAGAGACAGGG GGGGGGGGGGGGGG	Integrated DNA Technology
PCR_1B TCATCGGCTCGTATAATGTGTGG	Integrated DNA Technology
PCR_2A CAAGCAGAAGACGGCATACGAGATTGCCTTAGTCT CGTGGGCTCGG	Integrated DNA Technology
PCR_2B CAAGCAGAAGACGGCATACGAGATCTAGTACGGTCT CGTGGGCTCGG	Integrated DNA Technology
PCR_2C AATGATACGGCGACCACCGAGATCTACACCTAGAGA CCGGGGACTTATCAGCCAACCTGTTA	Integrated DNA Technology
Seq_primer CTAGAGACCGGGGACTTATCAGCCAAC	Integrated DNA Technology

Plasmids	Source
pEXG2-Δpa2541	This study
pEXG2-Δpa2536	This study
pEXG2-Δpa4323	This study
pEXG2-Δpa4320	This study
pEXG2-Δpa5114	This study
pEXG2-Δpa5114/pa5113	This study
pEXG2-Δpa3267	This study
pEXG2-Δpa5113	This study
pEXG2-Δpa5112	This study
pEXG2-Δpfl_rs01995	This study
pEXG2-pa2541_vsv-g	This study

pEXG2- <i>pa4323</i> <i>vsv-g</i>	This study
pEXG2- <i>pa5114</i> <i>vsv-g</i>	This study
pEXG2- <i>pa5113</i> <i>vsv-g</i>	This study
pUC18-Tn7t-pBAD-araE	42
pUC18-Tn7t-pBAD-araE- <i>pa2541</i>	This study
pUC18-Tn7t-pBAD-araE- <i>pa4323</i>	This study
pUC18-Tn7t-pBAD-araE- <i>pa5114</i>	This study
pUC18-Tn7t-pBAD-araE- <i>pfl</i> <i>rs01995</i>	This study
pUC18-Tn7t-pBAD-araE- <i>i35</i> <i>rs27920</i>	This study
pUC18-Tn7t-pBAD-araE- <i>pspto</i> <i>rs26695</i>	This study
pUC18-Tn7t-pBAD-araE- <i>ta05</i> <i>rs00690</i>	This study
pTNS3	42
pJRC115- <i>BTH</i> <i>II0090</i> ^{S264A}	This study
pJRC115- <i>BTH</i> <i>I3226</i> ^{S264A}	This study
pJRC115- <i>BTH</i> <i>I2698</i> ^{S267A}	This study
pJRC115- <i>BTH</i> <i>I2701</i> ^{S267A}	This study
pJRC115- <i>ΔBTH</i> <i>I2691</i>	This study
pJRC115- <i>ΔBTH</i> <i>I3225-8</i>	This study
pJRC115- <i>ΔBTH</i> <i>II0089-94</i>	This study
pUC18T-miniTn7T-Tp-PS12-mCherry	43

Supplemental Table 6. Internal standards and parameters used in lipidomic analysis

Internal standards used		
Compound formula	Compound Name	Alternative name
C20H41O9P	LysoPG(14:0)	
C24H49O9P	LysoPG(18:0)	
C34H67O10P	PG(14:0/14:0)	
C46H91O10P	PG(20:0/20:0), i.e. diphytanoyl PG	
C19H40O7PN	LysoPE(14:0)	
C23H48O7PN	LysoPE(18:0)	
C29H58O8PN	PE(12:0/12:0)	
C45H90O8PN	PE(20:0/20:0), i.e. diphytanoyl PE	
C66H120O17P2	CL(57:4)	14:1(3)-15:1 CA
C70H134O17P2	CL(61:1)	15:0(3)-16:1 CA
C89H166O17P2	CL(80:4)	22:1(3)-14:1 CA

Mass spectrometry global parameters on Waters Xevo TQS mass spectrometer	
Parameter	Value
Cycle time	Automatic
Source temperature (°C)	150
Desolvation temperature (°C)	250
Cone gas flow (L/h)	150
Desolvation gas flow (L/h)	650
Collision gas flow (mL/min)	0.14
Nebuliser gas (Bar)	7
LM 1 Resolution	2.8
HM 1 Resolution	14.8

Mass spectral acquisition and data processing parameters
Acquisition parameters

Compound	Function	m/z range	Start/end time (min)	Scan duration (s)	Ionization mode	Cone voltage (V)	Collision energy (V)	Total scan time (min)
PG	Neutral Loss of 189.04	680 to 880	1.6 to 5	2	ES+	30	8	3.4
LPE, PE	Neutral Loss of 141.02	422 to 922	1.6 to 5	5	ES+	40	20	3.4
LPG	Parents of 152.9	420 to 570	5.2 to 10	0.75	ES-	30	38	4.8
CL, MLCL	Parents of 153	865 to 1572	1.6 to 30	4.7	ES-	40	75	28.4

Data processing parameters		
Subtraction	Smooth mean	Centroid mid peak width at half height (all top 50%)
1, 40, 0.01	2 x 0.4	2
1, 40, 0.01	2 x 0.4	2
1, 40, 0.01	1 x 0.6	5
1, 40, 0.01	2 x 0.6	5

Supplemental Table 7. Transposon sequencing data summary

Growth experiment	Mutant pool pre-competition	Pool with WT <i>B. thai</i> - rep 1	Pool with Δ T6S <i>B. thai</i> - rep 1
fastq file name	tn_mutant_pool.fastq	pool_v_wt_rep1.fastq	pool_v_deltaT6_rep1.fastq
Total reads	515,434	5,788,728	6,452,899
Trimmed (valid Tn prefix)	515,293	5,786,427	6,450,594
Mapped	350,923	4,666,597	5,283,645
Mapped to TA sites	349,915	4,634,942	5,241,672
TA_sites	94,404	94,404	94,404
TAs_hit	50,348	57,644	60,331
Max reads per TA site	324	9,519	5,886
Mean reads per hit TA site	6.9	80.4	86.9

Pool with WT <i>B.thai</i> - rep 2	Pool with Δ T6S <i>B.thai</i> - rep 2	Pool with <i>tle3</i> ^{S264A} <i>B. thai</i>	Pool with <i>ΔcolA</i> <i>B. thai</i>
pool_v_wt_rep2.fastq	pool_v_deltaT6_rep2.fastq	pool_v_tle3.fastq	pool_v_colA.fastq
411,515	720,133	3,226,978	3,130,545
411,401	719,895	3,225,816	3,129,574
266,466	481,466	3,024,047	2,938,318
265,661	479,769	2,997,466	2,922,995
94,404	94,404	94,404	94,404
46,500	53,148	59,145	58,101

669	447	3,484	3,568
5.7	9.0	50.7	50.3